2006

The Relationship Between Lactic Acid, Reactive Oxygen Species and the Hypoxia-Induced Acidification Seen in Chemosensitive Neurons of the Nucleus Tractus Solitarius (NTS)

Trevor Downing
Wright State University

THE RELATIONSHIP BETWEEN LACTIC ACID, REACTIVE OXYGEN SPECIES AND THE HYPOXIA-INDUCED ACIDIFICATION SEEN IN CHEMOSENSITIVE NEURONS OF THE NUCLEUS TRACTUS SOLITARIUS (NTS)

A thesis submitted in partial fulfillment
of the requirements for the degree of
Master of Science

By

TREVOR MICHAEL DOWNING
B.S., Wright State University, 2003

2006
Wright State University

WRIGHT STATE UNIVERSITY

SCHOOL OF GRADUATE STUDIES

June 20, 2006

I HEREBY RECOMMEND THAT THE THESIS PREPARED UNDER MY SUPERVISION BY Trevor Michael Downing ENTITLED The Relationship Between Lactic Acid, Reactive Oxygen Species and the Hypoxia-Induced Acidification Seen in Chemosensitive Neurons of the Nucleus Tractus Solitarius (NTS) BE ACCEPTED IN PARTIAL FULFILLMENT OF THE REQUIREMENTS FOR THE DEGREE OF Master of Science.

_____

Jay B. Dean, Ph.D.
Thesis Director

_____

Timothy C. Cope, Ph.D.
Department Chair

Committee on
Final Examination

_____

Robert W. Putnam, Ph.D.

_____

Larry Ream, Ph.D.

_____

Joseph F. Thomas, Jr., Ph.D.
Dean, School of Graduate Studies

ABSTRACT

Downing, Trevor Michael. M.S., Department of Neuroscience, Cell Biology and Physiology, Wright State University, 2006. The relationship between lactic acid, reactive oxygen species (ROS) and the hypoxia-induced acidification seen in chemosensitive neurons of the nucleus tractus solitarius (NTS).

The NTS is one of many sites of chemoreception which means that it consistently responds to changes in carbon dioxide and pH. NTS neurons also acidify approximately 0.13 pH units in response to hypoxia. The exact cause of this acidification is under debate. To study the cause of this acidification, slices of medullary brainstem (300µm) were taken from neonatal Sprague-Dawley rats (P1-P12) and loaded with one of two fluorescent probes. The two probes were BCECF and DHE which measure intracellular pH (pH_i) and superoxide levels, respectively. During the experiments, slices were exposed to a control hypoxic bout followed by a hypoxic bout in conjunction with a variety of drugs. Studies of the NTS with fluorocitrate (FC) and 4-hydroxycinnamate (4-Cinn) did not show a significant alteration in the hypoxia-induced acidification compared to the control hypoxic exposure. Studies with fluorocitrate and 4-Cinn were repeated in the retrotrapezoid nucleus (RTN) for control purposes due to differences in the quantity of glial cells. The studies using oxygen-glucose deprivation (OGD) showed a decrease in the ΔpH_i by ~25% in a portion of the neurons of the NTS (n=56) but in the whole population of neurons studied (n=140), no significant effect was seen. The compound iodoacetate produced the most robust blunting of the hypoxia-induced acidification and decreased the response by ~53% with a mean ΔpH_i of 0.08±0.005 compared to the control response of 0.18±0.007 (n=39). Results from the studies using the superoxide probe

DHE showed an increase in the levels of reactive oxygen species (ROS) of 12.9±0.7 arbitrary fluorescence units (afu) during the hypoxic exposure prior to reoxygenation. The two ROS scavengers melatonin and manganese(III)tetrakis(1-methyl-pyridyl)porphyrin pentachloride (MnTMPyP) both reduced the increase in ROS by ~30%. ΔROS = 8.6±0.56afu with melatonin compared to a control hypoxic response of 12.8±0.73afu (n=39) and ΔROS = 12.4±1.15afu with MnTMPyP compared to a control response of 17±1.15afu (n=41). ΔpH_i response in the NTS during exposure to hypoxia in conjunction with a cocktail of melatonin and MnTMPyp caused a reduction in the acidification of 30% with ΔpH_i = 0.12±0.001afu compared to the control response of 0.15±0.007afu (n=54). In conclusion, the hypoxia-induced acidification seems to be due to lactate production which is proposed to come from neuronal sources as the glial source of lactate was ruled out with the FC and 4-Cinn studies.

TABLE OF CONTENTS

LIST OF FIGURES

Page

ACKNOWLEDGEMENTS

To

…

CHAPTER I

INTRODUCTION

The ability of mammals to alter breathing in response to varying metabolic demands relies on the chemoreceptors. These chemoreceptors are located in numerous regions throughout the body. The chemoreceptors found at the bifurcation of the common carotid arteries are commonly known as the peripheral chemoreceptors and respond primarily to reduced arterial O_2. The central chemoreceptors are predominantly CO_2 receptors and are found in several regions of the brainstem.

These chemoreceptors are proposed to be a group of neurons that respond to a stimulus by increasing their rate of firing and in doing so, can alter breathing patterns to maintain homeostatic blood gas levels. Several stimuli have been proposed as the primary stimulus for the central chemoreceptors and these include changes of CO_2, intracellular and extracellular pH, carbonic anhydrase and HCO_3^-. Although some of the central chemoreceptor regions have been shown to respond to oxygen, the majority of the regions do not. However, hypoxia or low levels of oxygen will consistently acidify neurons of the nucleus tractus solitarius (NTS), a well known central chemoreceptor region. Using brainstem slices from this region, the purpose of my thesis was to address this hypoxia-induced acidification and attempt to identify the cause of it. In some cases, studies of another well known central chemoreceptor region, the retrotrapezoid nucleus (RTN), were done for purposes of control. I will focus on the impact of glial and neuronal metabolism and the production of reactive oxygen species (ROS) as potential causes for the hypoxia-induced acidification.

CHAPTER II

LITERATURE REVIEW

The goal of this thesis is to determine the primary cause of the hypoxia-induced acidification seen in the neurons of the nucleus tractus solitarius (NTS) in a slice of rat brainstem. I plan to do this by focusing on two aspects of neuronal physiology. The first is the production of lactic acid during anaerobic metabolism and the second is the production of ROS during changes in the level of oxygen. In addition, I will illustrate that another chemosensitive region, the retrotrapezoid nucleus (RTN), will also acidify in response to hypoxia and I will use the RTN to compare the response to that of the NTS.

Hypoxia and clinical manifestations.

Hypoxia, by definition, is the deficiency of oxygen at the level of the tissues. Hypoxia manifests itself clinically in numerous disease states which can be grouped into a few categories. Hypoxia can result from ischemia which is inadequate blood flow to the tissues. This is most commonly seen in cerebral strokes resulting from clot formation. Ischemia, and furthermore hypoxia, have been shown to cause significant sensorimotor impairment in rats (MacGregor et al., 2003). If severe enough, the ischemia can lead to cerebral edema which has been identified as the primary cause of patient mortality in cerebral strokes. The cerebral edema can result from numerous factors which include: glutamate receptor activation and subsequent Na^+ ion influx leading to swelling (Brahma et al., 2000), increased intracellular Ca^{++} loading, which can result in astrocyte swelling, and increased ROS production resulting in edema (Brahma et al. 2000)

Hypoxia could also result from a hypoventilation syndrome originating in the neurons responsible for the control of breathing such as in sleep apnea (Katz-

Salamon, 2004). Sleep apnea is a condition whereby individuals will stop breathing for short periods of time during sleep which leads to a condition known as intermittent hypoxia. Intermittent hypoxia is characterized by short periods of hypoxia followed by periods of reoxygenation (Lavie, 2005). As of yet, the exact mechanism causing sleep apnea has not been identified. Disorders of breathing such as sleep apnea have been implicated as the cause of sudden infant death syndrome (SIDS) which is the leading cause of death of infants between 2 weeks and 1 year of age (Morris et al., 2003). Numerous studies have been done examining the effects of the hypoxic bouts that result from the disturbance in breathing. The list of pathological conditions that result from intermittent hypoxic bouts is long and includes such deleterious conditions as increased systemic hypertension resulting from increased sympathetic tone (Fletcher, 2003, Narkiewicz et al., 2003), increased risk of myocardial infarction in rat heart tissue (Joyeux-Faure et al., 2005), and atrophy of hippocampal tissue in humans (Gale et al., 2004), which can lead to neurocognitive defects associated with learning and memory. The neurocognitive defects can be attributed to increased cellular apoptosis mediated by increased quantities of reactive oxygen species as shown by Gozal and others (Xu et al., 2004). All of these symptoms are debilitating and can potentially lead to various neuropathologies and ultimately, death.

Other incidences of hypoxia can result from chronic obstructive pulmonary diseases (COPD), which include asthma, emphysema and bronchitis. In these cases, a ventilation defect in the lungs results in a deficiency in oxygen exchange through the alveoli into the blood which results in hypoxia of the tissues throughout the body

(Agusti, 2005). Hypoxia could also be due to an environmental condition where, for instance, an individual moves to a higher altitude and the partial pressure of oxygen is reduced in the atmosphere. Hypoxia can result from histotoxic mechanisms, which essentially means poisons to the tissues; specifically, a disruption of either O_2 transport in the blood or O_2 utilization by the mitochondria. These poisons vary in mechanism. For instance, carbon monoxide (CO) competes with oxygen to bind to hemoglobin and in doing so, prevents oxygen from reaching the tissues. In addition to this, CO will bind to cytochromes involved in oxidative phosphorylation and prevent aerobic metabolism. Depending on the severity of the CO poisoning, a variety of symptoms can result. The symptoms could range from syncope (a brief loss of conciousness due to temporary lack of oxygen to the brain), pulmonary edema and myocardial ischemia to more severe conditions of coma and seizures (Tibbles and Edelsberg, 1996). Another example of a histotoxic poison is cyanide which similarly blocks oxidative phosphorylation and even though oxygen can reach the tissues, it cannot be used as an electron acceptor at the end of electron transport. For all the aforementioned reasons, hypoxia is not beneficial for the body.

Anaerobic metabolism and lactic acid production

The direct effect of hypoxia is to force the cell into anaerobic metabolism and the production of lactic acid. In the presence of oxygen, glucose is completely broken down into CO_2 and H_2O in order to yield a high amount of ATP. However, without oxygen, the cell cannot completely break down glucose because oxidative phosphorylation cannot proceed without oxygen. In this case, the cell must revert to anaerobic metabolism, whereby glucose is broken down incompletely into lactic acid.

This process generates a lesser amount of ATP so that during acute hypoxic bouts, the cell still has a small amount of energy. Once oxygen is restored, this lactic acid can then be sent through the normal glucose enzymatic pathways to generate more ATP.

All cells of the body will respond to hypoxia in this manner and this includes the neurons and glial cells of the brain. What is interesting to note is that glial cells in the brain have been shown to produce lactate under normal aerobic conditions, which is referred to as aerobic glycolysis (Walz and Mukerji, 1988). The metabolism of lactate and glucose in neurons and glial cells of the brain is particularly interesting because of how these two cell types interact to effectively distribute these two substrates based upon energy requirements. During normal metabolism, it has been estimated that neurons and glial cells account for, respectively, 90% and 10% of the energy requirements in the brain (Attwell et al., 2001). Interestingly, during these same conditions, the glucose supplied to the brain is equally distributed between neurons and glial cells (Nehlig et al., 2004). If the neurons account for 90% of energy demands but glucose is evenly distributed, this suggests that the glial cells are breaking the glucose down into a metabolic intermediate, perhaps lactate, and shuttling it over to the neurons to assist with increased metabolic demand. Evidence for this theory is supported by a recent study on rat vagal nerves and their associated Schwann cells. Results from the study show that a large percentage of glucose designated for the nerve is utilized by schwann cells to produce a metabolic intermediate that is then released and taken up by the neuron (Vega et al., 2003).

Based upon these aforementioned studies, it can be concluded that glial cells supply neurons with additional metabolic substrate to help with the increased

metabolic demand of neurons. The argument for lactate as this metabolic substrate is strengthened by a study that showed neurons will selectively increase their uptake of lactate even in the presence of high amounts of glucose (Smith et al., 2003). The majority of the energy demand in neurons seems to come from firing action potentials. Maintaining Na^+/K^+ gradients with ATPases accounts for most of the energy used by the neuron. Glial cells however, do not fire action potentials and so this suggests that their metabolic demand is less than that of neurons. To further extrapolate this idea, it can be expected that when neurons increase their rate of firing, they increase metabolic demand and as a result glial cells would be expected to increase their supply of lactate. Evidence of this idea came in a study performed by Pellerin and others, whereby they showed that glutamate increases the breakdown of glucose and the production of lactate in glial cells (Pellerin et al., 1994). In addition to this, another study shows that glutamate increases the uptake of glucose into glial cells significantly (Loaiza et al., 2003). Numerous studies supporting this theory are summarized in a comprehensive review written by Pellerin and others (Pellerin et al., 2004).

In summary, it seems that the glial cells are producing lactate under aerobic conditions and this lactate is being used by neurons as an additional energy source to glucose during periods of increased metabolic demand. What is interesting to note however, is that this glial lactate shuttle mechanism is not beneficial to neurons during hypoxia. The main reason for glial cells to shuttle lactate to neurons is to allow the neuron to use the lactate for the TCA cycle and oxidative phosphorylation to generate large amounts of ATP. However, without oxygen, the neuron would be

unable to do this and so the lactate would essentially be useless. Furthermore, the lactate would more than likely be detrimental to the neuron due to the fact that during hypoxic conditions, the neuron will need to produce it's own lactate to generate small amounts of ATP. High quantities of lactate from the glial cells in this scenario will inhibit the neurons ability to produce lactate and ATP. A portion of my study will be dedicated to focusing on glial cell lactate as a source of the neuronal acidification.

Lactate is grouped with a few other substrates into a group known as monocarboxylates, which are not significantly lipid soluble. This suggests that monocarboxylates must require a transporter to be moved into and out of the cell. In other words, in order for glia and neurons to exchange lactate they both must have a transporter within the membrane. A large family of 14 monocarboxylate transporters (MCT) has been characterized. Of these, only MCT1, MCT2 and MCT4 have been found in the brain. MCT1 is specifically found on astrocytes, whereas MCT2 seems to be the transporter located on neuronal cells (Pierre et al., 2000) (Figure 1.). These MCT transporters have been characterized in other tissues for quite some time and seem to cotransport lactate with protons into neurons or out of glial cells (Schneider et al., 1993).

The evidence of these transporters allow for a novel approach in studying this interaction between glial cells and neuronal cells. The uptake of lactate by neurons with the MCT2 transporter theoretically should acidify the interior of the neuron due to the cotransport of lactate with protons. As a result of these findings, intracellular acidifications could potentially be related to the movement of lactate. A portion of my research will use a specific inhibitor of these transporters to determine whether there

is a relationship between the intracellular acidification seen in neurons of the nucleus tractus solitarius (NTS) during a hypoxic bout and these MCT transporters.

Glial cells have a variety of functions other than presumably producing lactate for neurons. During periods of high neuronal firing activity, extracellular K^+ will naturally increase due to the outflow of potassium in order for the neuron to repolarize. One potential problem of hyperkalemia, or high extracellular K^+, is that it causes a depolarization of the neuron's resting membrane potential which causes the neuron to be hyperexcitable. One important function of astrocytes, a subtype of glial cells, is spatial buffering of extracellular K^+ (Orkand, 1986). The astrocyte sequesters the K^+ in order to prevent hyperkalemia and protect the neuron from hyperexcitability.

Another important function of glial cells is determining the final position of a neuron within the brain. Glial cells have prearranged positions within the cortex and send out radiating glial processes which neurons attach to and move to their final destination (Hatten, 1990). In addition to determining the final position of neurons, glia are also responsible for taking up excitatory neurotransmitters such as glutamate (Erecinska and Silver, 1990) and inhibitory ones such as GABA (Levi et al., 1986). The purpose of this function is to prevent such pathological situations as the excitotoxicity that can occur as a result of high levels of neurotransmitters in the extracellular fluid (ECF). The glial cells commonly known as oligodendrocytes and Schwann cells have a function in myelin formation, the purpose of which is to speed action potential conduction along axons.

FIGURE 1. Schematic indicating the astrocyte neuron lactate shuttle. Although neuronal metabolism is significantly higher than that of glial cells, the uptake of glucose is approximately equal between the two compartments. As the figure indicates, the glial cells transport lactate in conjunction with protons through the MCT1 transporter into the interstitium whereby the neurons will then take the lactate up through a MCT2 transporter. This lactate is then converted into pyruvate which is then fed into the TCA cycle and further processed through oxidative phosphorylation to yield ATP (diagram modified from Pellerin et al., 2004).

FIGURE 1.

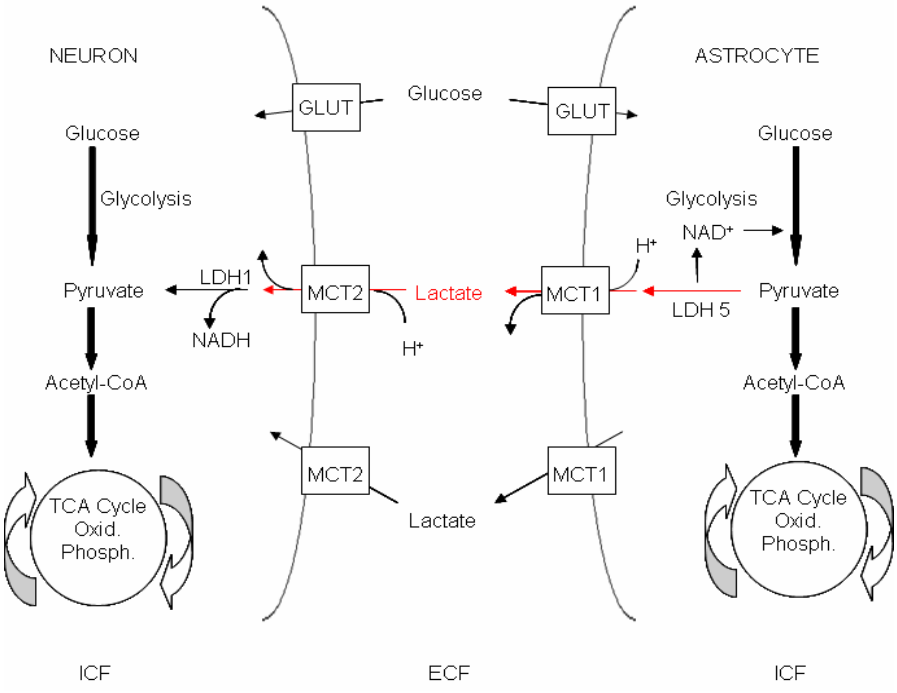
NEURON
ASTROCYTE
GLUT
Glucose
GLUT
Glucose
Glucose
Glycolysis
Glycolysis
NAD+
H+
LDH1
MCT2
Lactate
MCT1
Pyruvate
Pyruvate
NADH
LDH 5
H+
Acetyl-CoA
Acetyl-CoA
MCT2
MCT1
TCA Cycle
Oxid.
Phosph.
Lactate
TCA Cycle
Oxid.
Phosph.
ICF
ECF
ICF

Finally, glial cells have an important role in the buffering of ECF pH (Largo et al., 1996; Deitmer et al., 1996). This function is most pertinent for this study because we used drug compounds which will compromise the ability of the glial cell to maintain ECF pH. If the glial cell is unable to control ECF pH, this will inevitably lead to a change in the neuronal intracellular pH. This change in neuronal pH can be monitored allowing us to summise that the compound was working adequately. This theory is based upon studies performed by Erlichman and others whereby they exposed slices of the RTN region to fluorocitrate and noted an acidification of the ECF pH (Erlichman et al., 1998). Although the source of this acidification is unknown, the study indicates that glial cells have a role in controlling ECF pH.

Functions of Central Chemoreceptors

I am particularly interested in the neurons of the NTS because they are proposed to be one of the sites of CO_2-chemosensitivity, and are reported to also be highly-sensitive to *increased* tissue O_2 tension (P_{tO_2}) (Mulkey et al., 2003). During everyday life, it is imperative that the body is able to alter its rate of ventilation in order to satisfy the oxygen needs of all the cells of the body. For instance, during times of exercise, the metabolic rate of cells is increased and therefore an increase in the rate of breathing is required in order to supply an adequate amount of oxygen. As a result of this, there are regions in the body that are able to detect levels of blood gases and these regions are associated with neurons with efferent fibers that project to the diaphragm to alter ventilation. The regions are commonly known as central CO_2-chemoreceptors (Figure 2.).

FIGURE 2. Diagram showing the projections of the phrenic nerve from cervical spinal nerves (C3,C4,C5) to innervation of the diaphragm. In addition, a dorsal view of the pontine and medullary brainstem regions with the cerebellum removed is indicated on the right. The NTS region is shown as the solitary tract on the right of the figure along with efferent motor projections as the bulbospinal tract initially but then through the ventral columns and finally as the phrenic nerve.

FIGURE 2.

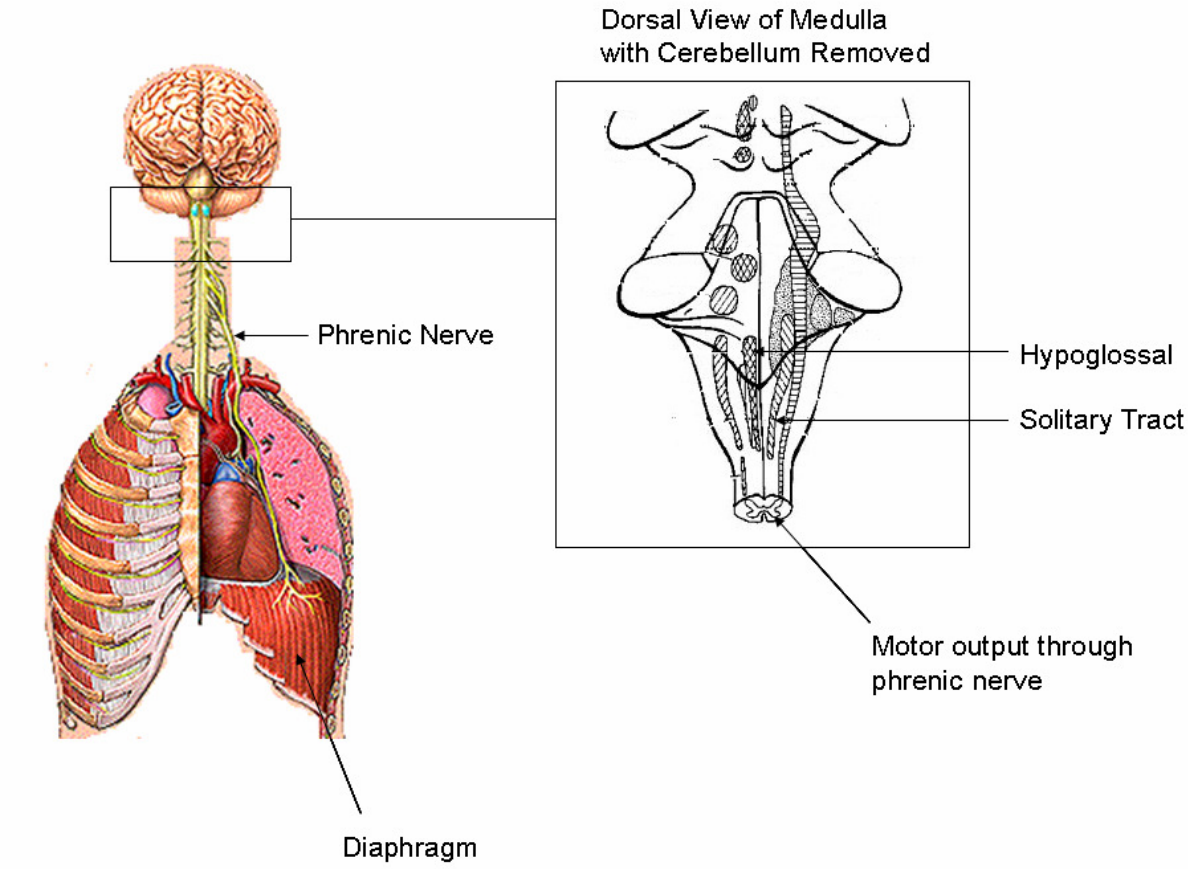
Dorsal View of Medulla
with Cerebellum Removed
Phrenic Nerve
Hypoglossal
Solitary Tract
Motor output through
phrenic nerve
Diaphragm

According to Putnam and others, a chemosensitive neuron is defined as a neuron that responds to changes in CO_2/H^+, has axonal projections to a respiratory control center and can ultimately lead to a change in ventilation when focally acidified (Putnam et al., 2004). In this case, numerous regions have been identified that contain chemosensitive neurons. The carotid body located at the bifurcation of the common carotid artery contains the peripheral chemoreceptors which respond to arterial levels of P_{O_2}, P_{CO_2} and pH (Gonzalez et al., 1992). The central chemoreceptors have been identified in a variety of regions in the brainstem, one of which is the NTS (Nattie, 1999). The central chemoreceptors respond to arterial and cerebrospinal fluid (CSF) P_{CO_2} and pH. The exact mechanism whereby these chemoreceptors change ventilatory activity is still under debate. Studies show that increasing P_{CO_2} will stimulate neurons of the solitary complex which includes neurons of the nucleus tractus solitarius and the dorsal motor nucleus neurons (Dean et al., 1989) (Figure 3.). Other regions that respond to increased P_{CO_2} include neurons of the medullary raphe (Richerson, 1995), locus coeruleus (Filosa et al., 2002), Pre-Bötzinger complex (Solomon et al., 2000), neurons of the retrotrapezoid nucleus (Guyenet et al., 2005, Ritucci et al., 2005) and cultured neurons from the ventral medulla (Wellner-Kienitz et al., 1998). Interestingly, some of these neurons will respond to changes in pH when P_{CO_2} is kept constant, like those in the ventral medulla (Miles, 1983) and the locus coeruleus (Filosa et al., 2002).

Based upon these aforementioned studies and many others, it seems the most popular proximal stimulus for these chemoreceptors is decreased pH_i. Other factors that have been suggested as part of the chemosensitive signal include changes of pH_o,

FIGURE 3. Sagittal section of the rat brainstem showing currently identified regions of central chemosensitivity (Nattie, 2000). Shaded regions are those implicated in central chemosensitivity whereas lighter regions are provided for anatomical landmark purposes. Regions are labeled as follows; AMB: nucleus ambiguus, FN: fastigial nucleus, LC: locus coeruleus, NTS: nucleus of the solitary tract, Pn: pontine nucleus, RTN: retrotrapezoid nucleus, rVRG: rostral ventral respiratory group, SO: superior olive, VII: facial nucleus, and 7N: root of the facial nucleus.

FIGURE 3.

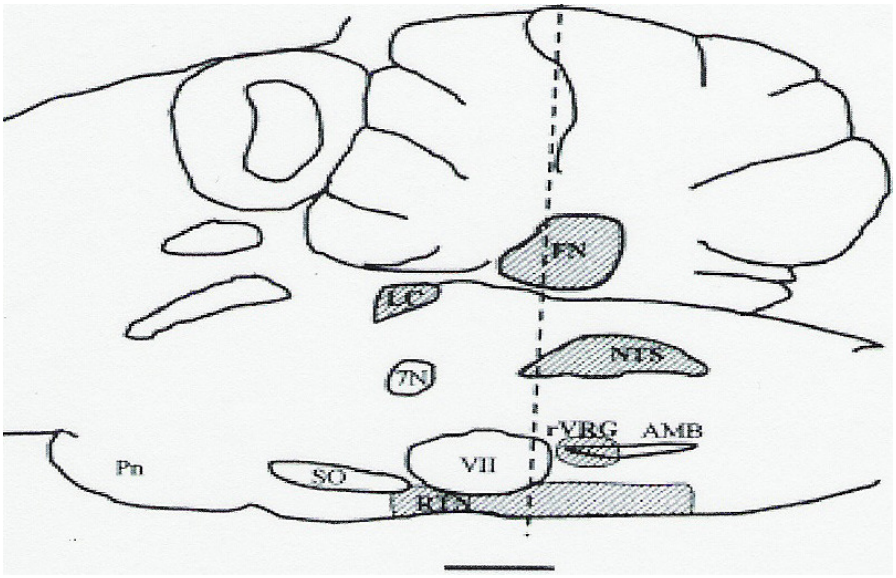

calcium, bicarbonate, carbonic anhydrase, gap junctions, oxidative stress and glial cells (for review consult Putnam et al., 2004). Regardless, we can say unequivocally that chemosensitive neurons have been shown to respond to changes in pH. This pH change can be related to CO_2 due to the fact that CO_2 readily diffuses into the cell whereby it combines with water to produce bicarbonate and protons, in which case, the increase in protons acidify the interior of the cell. Studies have also shown however, that central chemoreceptors will respond to CO_2 and pH independently from one another but the additive effect will produce the most robust response (Harada et al., 1985).

It is interesting to note that hypoxia produces an intracellular acidification similar in magnitude to that of CO_2 (Chambers-Kersh et al., 2000). The proposed mechanism of this is assumed to be increased lactic acid production under anaerobic conditions. That being the case, it would be assumed that this acidification, which occurs under hypoxic conditions, would also stimulate the central chemoreceptors through a change in pH. Very few studies have shown these central chemoreceptors to respond to hypoxia and subsequently the accepted theory has been that they do not respond to hypoxia.

The term that has been assigned to this phenomenon is commonly known as the hypoxia paradox (Nattie, 1998). The hypoxia paradox essentially encompasses the idea that central chemoreceptors will respond to a decrease in pH_i with increased firing rate. In most cases however, they do not increase firing rate in response to decreased pH_i in response to hypoxia. The suggested explanation for this paradox involves the lack of ATP and a particular K^+ channel located in the neuronal

membrane. Most neurons have been shown to contain a K^+ channel in their membranes that opens in response to decreased levels of ATP (Kiluk et al., 2002; Ballanyi, 2004). The logic behind this channel is that when the neuron is low on ATP, one of it's primary objectives is to reduce metabolic demand to conserve energy. By opening a K^+ channel in the membrane, the neuron will hyperpolarize and essentially become quiescent or silent. This is the reverse response of what happens during an acidification induced by hypercapnea or increased CO_2 which increases the firing rate of these neurons.

Regardless, a few studies have shown certain chemosensitive neurons do respond to hypoxia. One third of the neurons of the NTS have been shown to depolarize in response to hypoxia (Pascual et al., 2002) and neurons of the pre-Bötzinger complex have also been shown to respond to hypoxia (Solomon et al., 2000). However, in an anesthetized animal with the peripheral chemoreceptors removed, the central chemoreceptors do not respond to hypoxia (Kiwull-Shone and Kiwull, 1992). A few studies have suggested that if the peripheral chemoreceptors are left intact and perfused separately, there is a ventilatory response to brain hypoxia (Biscard et al., 1995; Smith et al., 1993) but it is generally accepted that central chemoreceptors do not respond to hypoxia unless under chronic life threatening conditions in which case hypoxia will elicit a gasping response which is proposed to come from the pre-Bötzinger complex (Neubauer et al., 2004)

Hyperoxic treatment of clinical manifestations and reactive oxygen species

As previously established, the effects of hypoxia are widespread and in some cases can be treated clinically by administering either normobaric or hyperbaric

hyperoxia. Hyperoxia is not a beneficial treatment in all cases of hypoxia, one of which includes ischemia. Assuming the ischemic incident is due to a blockage, raising the P_{O_2} will not alleviate the condition unless significant collateral circulation around the blockage is present. However, a large number of hypoxic conditions can be treated with hyperoxia such as CO poisoning, COPD and decreased tissue P_{O_2} due to altitude conditions. Normobaric hyperoxia would essentially encompass breathing greater than 21% oxygen at normal atmospheric pressure. Hyperbaric hyperoxia (HBO) on the other hand is breathing higher than 21% oxygen—usually pure oxygen—at higher than normal atmospheric pressure, up to a maximum of 3 atmospheres absolute (ATA) pressure. By raising the atmospheric pressure, the partial pressure of oxygen is increased significantly above those levels that could be achieved at normal atmospheric pressure.

In addition to treating hypoxia, hyperoxia has been shown to treat a wide variety of conditions. It has been shown to be clinically beneficial in the treatment of bacterial infections (Knighton et al., 1986). Hyperoxia ensures that a sufficient supply of oxygen is delivered to the neutrophils which use the oxygen to generate oxygen free radicals to destroy bacteria. HBO has also been used in treating some types of anaerobic infections such as Clostridium perfringens (Hill and Osterhout, 1972) and other aerobic infections such as Pseudomonas (Muhvich et al., 1989). In the latter case, hyperoxia was used as a supplemental therapy to enhance the effects of certain antibiotics.

Normobaric and hyperbaric hyperoxia are also used for treatment of CO poisoning. There is conflicting data between normobaric and hyperbaric oxygen as to

which should be used in treatment. In addition to this, the outcome of the hyperoxic therapy is dependent on the severity of CO poisoning but hyperoxia has been shown to be beneficial in treating CO poisoning and reducing neurological sequelae (Thom et al., 1995 and Raphael et al., 1989).

Numerous studies have also been performed to determine whether HBO is beneficial in the treatment of ischemia induced strokes. Following occlusion of the middle cerebral artery, studies show that rats treated with HBO have reduced infarction of cerebral tissue and fewer neurological deficits compared to a control group (Yin et al., 2005). Interestingly, other studies have shown that in similar experiments where the middle cerebral artery is occluded, HBO can be beneficial if administered within 6 hours of the insult but actually detrimental to the patient if administered 12 hours after the insult (Badr et al., 2001). HBO has been shown to treat other conditions such as necrotizing fasciitis, Clostridial myonecrosis, refractory osteomyelitis, decompression sickness and radiation induced tissue injury (Tibbles and Edelsberg, 1996).

A large amount of research has shown hyperbaric hyperoxia to be very beneficial for a variety of ailments. However, even more studies have shown that there are damaging effects of hyperoxia. These deleterious effects have been attributed to increases in the production of reactive oxygen species (ROS) such as superoxide radicals ($\cdot O_2^-$) or hydroxy radicals ($OH\cdot$) and the production of reactive nitrogen species. ROS are actually produced in every day life in a variety of ways. Oxidative phosphorylation generally produces water as a byproduct of ATP production but also produces a small amount of ROS as a byproduct (Lee et al.,

2002). Another way cells can produce ROS is through the degradation of purine nucleotides during hypoxic conditions. Under hypoxic conditions, purine nucleotides are broken down into hypoxanthine and xanthine, which are then converted into uric acid by an enzyme known as xanthine oxidase (XO). In the process of producing uric acid, XO uses oxygen as the oxidant in the reaction and in so doing produces superoxide radicals ($\cdot O_2^-$). One other way cells produce ROS is through the respiratory burst reaction that is used by macrophages and granulocytes to destroy foreign cells such as bacteria. By using the enzyme NADPH oxidase, macrophages generate huge amounts of $\cdot O_2^-$ that is released from the cell to destroy bacteria (Hampton et al., 1998). For a more comprehensive review of these processes and reactions refer to Bergamini and others (Bergamini et al., 2004).

It is evident from some of the ways that cells use ROS that high levels of ROS are damaging. The damage to cells from ROS is generally due to hydroxyl radicals produced by the reaction between $\cdot O_2^-$ and hydrogen peroxide. The hydrogen peroxide comes from the combination of two $\cdot O_2^-$ radicals and so the damage can essentially be attributed to $\cdot O_2^-$. Large quantities of hydroxy radicals will damage unsaturated fatty acids found primarily in the cell membrane which essentially leads to increased cell lysis (Girotti., 1998). In addition to lipid damage, ROS is known to directly damage proteins by either direct modification of the protein backbone or oxidation of protein side chains. This could potentially lead to inactivation of a wide array of enzymes including those involved with mitochondrial electron transport (Andersson et al., 1998). Amino acids like cysteine and methionine can be directly oxidized by ROS in which case, this leads to altered biological activity of the

respective proteins that contain them (Bergamini et al., 2004). Nucleic acids are also susceptible to ROS damage that occurs when purine bases are modified and the glycosidic linkage broken. This will eventually lead to DNA strand breakage and is particularly prevalent in mitochondrial DNA due to its constant exposure to ROS from oxidative phosphorylation byproducts (Graziewicz et al., 2002).

It is a commonly believed theory that hyperoxia causes superoxide radicals (Chance et al., 1979) but what is relatively new in the field is the paradox of hypoxia increasing ROS. Recent studies show that exposing mice to prolonged periods of extreme hypoxia generates all the signs and symptoms of increased ROS and oxidative stress in skeletal muscle (Magalhaes et al., 2005). These signs include increased protein oxidation, mitochondrial dysfunction and depletion of normal cellular antioxidants, glutathione and vitamin E. Other studies have shown increased ROS during hypoxia. Becker and others showed an increased production of $\cdot O_2^-$ in cardiomyocytes during ischemia but prior to reoxygenation (Becker et al., 1999). Killilea and others showed increased ROS or reactive nitrogen species in pulmonary smooth muscle during hypoxia (Killilea et al., 2000). Promising research into hypoxia induced increases in ROS is currently being performed in our lab.

As previously stated, a common perception is that ROS increase during hyperoxia. However, we are suggesting that ROS increase during hypoxia and there is significant evidence in the literature to support this theory. The exact mechanism whereby this hypoxia induced increase in ROS occurs has not been identified. It has been shown that hypoxia disrupts the mitochondrial electron transport chain which in turn increases the production of ROS (Chandel et al., 2000). Chandel and others show

that the cytochrome complex III enzyme actually generates large quantities of superoxide within the mitochondrial matrix during varying levels of hypoxia. These studies were based upon others which show that complex III can produce ROS during normoxic conditions (Boveris et al., 1972, Turrens et al., 1985). The superoxide is proposed to escape into the cell where it acts as a message for the cell to produce hypoxia-inducible factor 1 which in turn stimulates the cell to produce a variety of gene products in order to counteract or respond to the hypoxic stress (Chandel et al., 2000). The gene products include such things as erythropoietin which increases the number of circulating erythrocytes, tyrosine hydroxylase which increases the quantity of dopamine in the carotid bodies and an angiogenic factor VEGF which stimulates growth of new capillaries. All of these gene products provide a mechanism to return adequate supplies of oxygen to region of concern. My intent is not to delve into the specifics of these biochemical mechanisms but merely to indicate that although common perception is that hyperoxia increases ROS, hypoxia is also able to do this.

Having established that hypoxia can increase ROS, a portion of my thesis is dedicated towards showing a relationship between increased ROS and the hypoxia induced acidification seen in neurons of the NTS. A large number of studies have shown that oxidative stress can acidify a variety of different cells. Studies with hydrogen peroxide have shown acidifications in rat cerebellar astrocytes and C6 glioma cells (Tsai et al., 1997), in human aortic endothelial cells (Hu et al., 1998), and in rat and human cardiac myocytes (Chao et al., 2002; Wu et al., 1996). In addition, our lab has shown neurons of the solitary complex to acidify in response to both chemical oxidants, Chloramine-T and N-chlorosuccinimide, and ROS

generators, hydrogen peroxide and dihydroxyfumaric acid (Mulkey et al., 2004). As of yet, the mechanism whereby ROS causes an intracellular acidification has not been identified, but a few possibilities can be suggested. There is some suggestion that oxidative stress causes oxidation of cysteine and methionine residues of the Na^+/H^+ exchanger which renders it unable to control intracellular pH (Mulkey et al., 2004, Hu et al., 1998). Another possibility of ROS causing a decrease in pH_i could involve ROS blocking oxidative phosphorylation. There is some evidence that oxidative stress increases lactic acid production in the CNS (Chan et al., 1982) and this could potentially be due to ROS blocking oxidative phosphorylation (Chance and Boveris, 1978). Mulkey and others have also suggested that perhaps hydrogen peroxide and oxidative stress increases the hydrolysis of ATP which leads to an increase in cytosolic hydrogen concentration. For a more detailed review of these mechanisms consult Mulkey et al. (2004).

In recap, the purpose of this thesis is to determine the cause of the hypoxia-induced acidification. I propose two sources for this acidification. The first is lactic acid produced by the neuron, the second is increased production of ROS during hypoxia which causes the acidification through mechanisms previously mentioned. In the process of studying these two aims, I will also show that neurons of the RTN acidify in response to hypoxia and that ROS can be generated during hypoxia as opposed to the reoxygenation portion following hypoxia.

CHAPTER III

HYPOTHESIS & SPECIFIC AIMS

AIM 1: To determine the cause of the acidification induced by hypoxia in the neurons of the nucleus tractus solitarius (NTS) in a slice of rat brainstem.

Hypothesis: **The neuronal intracellular acidification during hypoxia is due to increased lactic acid production.** To test this hypothesis, the following experiments will be run:

1a) Measure the pH_i response of neurons during hypoxia versus hypoxia with glucose deprivation (i.e. oxygen glucose deprivation, OGD). ***Rationale:*** Removing glucose from the solution removes the substrate necessary to produce lactic acid and in doing so should result in a blunting of intracellular acidification during hypoxia.

1b) Using the drug iodoacetate (IA), pH_i measurements during hypoxia versus hypoxia with IA will be made. ***Rationale:*** Iodoacetate will block neuronal and glial cell metabolism by blocking glyceraldehyde-3-phosphate dehydrogenase (GAPD) (Even et al., 1999) and in doing so, will prevent the production of lactic acid which will reduce the hypoxia-induced acidification.

1c) Intracellular pH (pH_i) changes will be monitored under hypoxic conditions versus hypoxia with fluorocitrate. Fluorocitrate will be used to block glial cell metabolism in brainstem slices, thereby blocking the production of lactic acid by the glial cells. ***Rationale:*** It has been suggested that glial cells transport lactate into the extracellular space for uptake by neurons to be used as substrate for energy production (Pellerin et al., 2004). We propose that during the neuronal hypoxia-induced acidification, glial cells transport lactate to the neurons and this will perhaps account for the acidification. These studies will

compare the pH_i response to hypoxia in two regions: the NTS (P1-P12), which does not contain significant amounts of glia at this particular age, and the retrotrapezoid nucleus (RTN), another CO_2-chemosensitive region, which is known to have high numbers of glial cells (Erlichman et al., 2004).

1d) pH_i changes will be monitored during hypoxia versus hypoxia with 4-hydroxycinnamate (4-Cinn). 4-Cinn is an inhibitor of the lactate/H^+ transporters found on glial cells and neurons. ***Rationale:*** A monocarboxylate transporter (MCT1) has been identified on glial cells, and it's function is to extrude lactate into the extracellular space. A similar monocarboxylate transporter has been identified on neurons (MCT2) and it's function is to take up lactate produced by glial cells. Using 4-Cinn at high enough concentrations to block both MCT1 and MCT2, the relationship between increased lactate production and the acidification induced by hypoxia will be determined.

AIM 2: To determine if intracellular acidification during hypoxia is due to increased production of reactive oxygen species (ROS). ***Hypothesis:*** **During hypoxic conditions, ROS production increases and contributes to intracellular acidification.** To test this hypothesis, the following three sets of experiments will be run:

2a) The ROS-sensitive fluorogenic probe, dihydroethidium (DHE), will be used to measure the effects of hypoxia and reoxygenation on the rate of production of ROS (specifically, superoxide) in neurons of the NTS.

Rationale: A paradox in neurobiology of oxidative signaling and stress is that a *decrease* in tissue P_{O_2} can *increase* production of ROS. Previous studies in

this lab have shown that chemical generators of ROS and pro-oxidants cause intracellular acidification of NTS neurons (Mulkey et al., 2004). These experiments test the provocative hypothesis that hypoxic cellular acidosis is caused by increased production of ROS.

2b) The effects of two ROS scavengers, melatonin (an antioxidant) and MnTMPyp (a superoxide dismutase mimetic), will be tested to determine if they blunt the hypothesized increase in ROS production during hypoxia. ***Rationale:*** These experiments will be further evidence that hypoxia increases production of ROS (superoxide).

2c) Likewise, the effects of melatonin and MnTMPyP will be tested to determine if they blunt the hypoxia-induced intracellular acidification. ***Rationale:*** These experiments would establish evidence for our hypothesis that hypoxia increases ROS production, which contributes to intracellular acidification.

CHAPTER IV

GENERAL METHODS

Slice preparation

Brainstem slices were prepared from Sprague-Dawley rats postnatal ages P1-P12. At this particular age, rat pups are poikilothermic and incapable of maintaining homeostatic body temperature. As a result, an accepted method of anesthesia is hypothermia with euthanasia by rapid decapitation. The portions of skull covering the brainstem and spinal cord were removed, revealing the dorsal section of the cerebellum, which was carefully brushed away. The brainstem was cut away slightly caudal to the inferior colliculi and transferred to a vibratome (Pelco Vibratome 1000). In order to yield slices containing the nucleus tractus solitarius (NTS), medullary brainstem slices (~300μm) were taken from the level of the obex and moving rostrally approximately 600-900μm (Figure 4). To yield slices containing the retrotrapezoid nucleus (RTN), pontine slices were taken beginning ~900μm caudal to the nuclei of cranial nerve VII (Figure 5). All slicing took place in artificial cerebrospinal fluid (aCSF, see below for composition) at 4-6°C and slices were incubated in aCSF at room temperature equilibrated with 95%O_2-5%CO_2 (pH ~7.45) for at least 1 hour to allow the slices to recover from slice damage.

Solutions

Standard aCSF contained (in mM) 5.0 KCl, 124 NaCl, 1.3 $MgSO_4$, 26 $NaHCO_3$, 1.24 KH_2PO_4, 10 glucose, and 2.4 $CaCl_2$ equilibrated with 95%O_2-5%CO_2, pH ~7.45 (at 37°C). Hypoxic solution was standard aCSF equilibrated with 95%N_2-5%CO_2, pH ~7.45 (at 37°C).

FIGURE 4. Images from the caudal NTS region of the medulla oblongata. The figure on the left is actual transverse medullary brainstem slices (~300µm) with the NTS indicated on the superior (dorsal) region of the lowermost slice (most caudal). Image on the right is a drawing of the same NTS slice with the NTS region shaded and demarcated.

FIGURE 4.

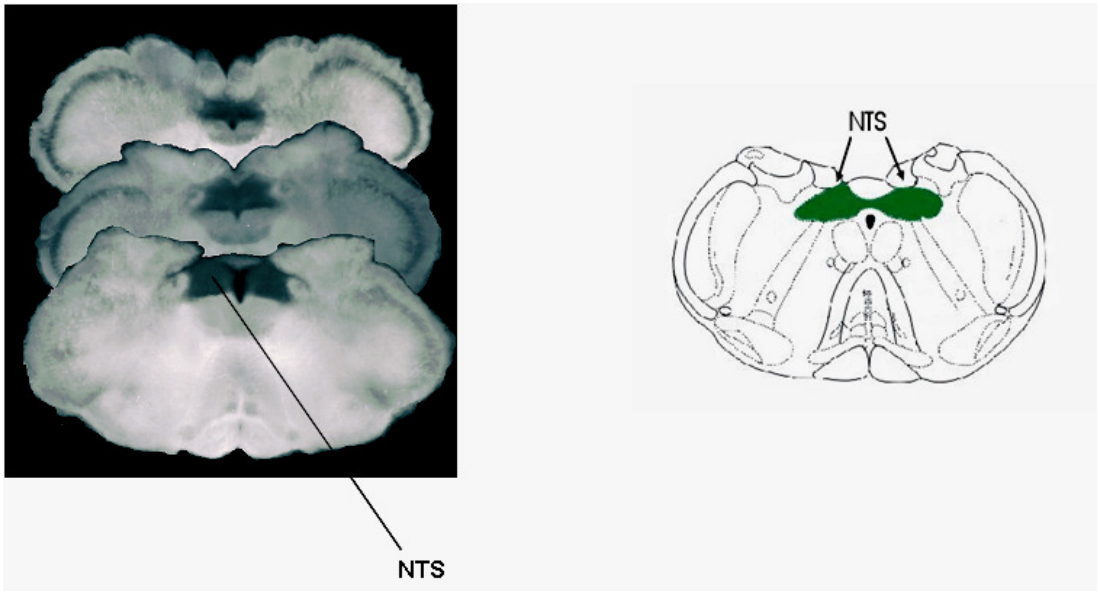

FIGURE 5. Images of pontine brainstem slices caudal to the nucleus of cranial nerve VII (facial nucleus). The image on the left is an actual transverse pontine slice with the RTN circled and indicated. The drawing on the right is of a similar pontine slice with RTN shaded and demarcated.

FIGURE 5.

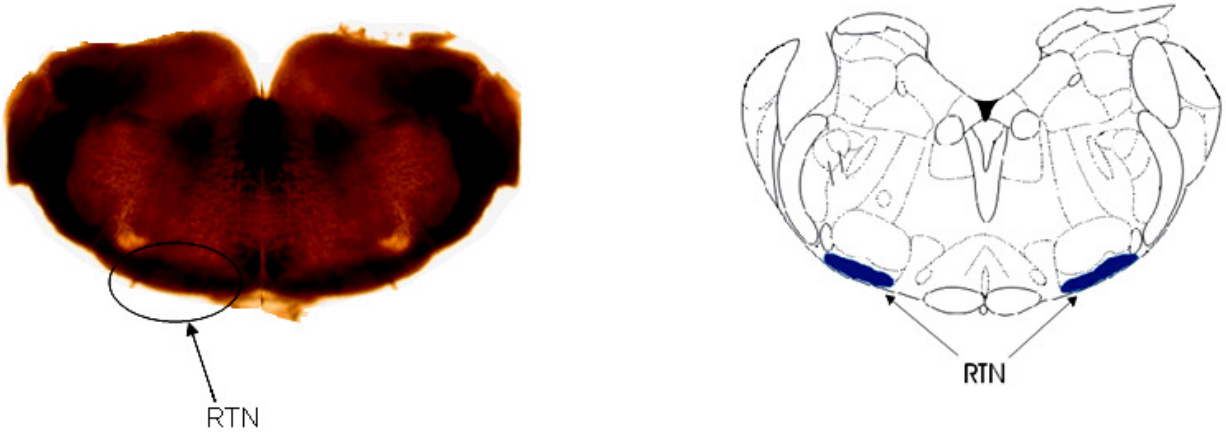

Experimental solutions

Oxygen-glucose deprived solution (OGD) was comprised of aCSF with 10mM glucose replaced isoosmotically with 10mM 2-deoxy-$_D$-glucose, which cannot be metabolized by cells, and equilibrated with 95%N_2-5%CO_2. Fluorocitrate (FC; Sigma-Aldrich), a potent glial toxin, was added directly to aCSF at a concentration of 1mM and NaCl concentration was reduced to maintain osmolarity. The compound 4-hydroxycinnamate (4-Cinn; Sigma-Aldrich) was purchased as α-cyano-4-hydroxycinnamic acid and was added to aCSF, which was titrated with either KOH or NaOH to a pH of ~7.45. A concentration of ~500μM was sufficient to block the monocarboxylate transporters found on both the neurons and glial cells (Erlichman et al., 2005). Iodoacetate was purchased from Sigma Aldrich as sodium iodoacetate and added to aCSF to yield a final concentration of 5μM. The compounds used to scavenge reactive oxygen species were melatonin (Mel; 100μM, Sigma) and manganese(III)tetrakis(1-methyl-pyridyl)porphyrin pentachloride (MnTMPyP; 25μM, Calbiochem). Melatonin is a non-specific antioxidant whereas MnTMPyP is a superoxide dismutase mimetic. Depending on the experiment, either melatonin or MnTMPyP were added directly to standard aCSF which was equilibrated with 95%O_2-5%CO_2 (pH ~ 7.45 at 37° C). In those experiments that involved both Mel and MnTMPyp, the compounds were both added to standard aCSF at concentrations of 100μM and 25μM, respectively.

BCECF-AM loading

The pH sensitive probe 2',7'-bis(carboxyethyl)-5(6)-carboxyfluorescein (BCECF) was used for the purposes of measuring pH_i. BCECF-AM is the

acetoxymethyl ester form of BCECF and is hydrophobic which means BCECF-AM can readily permeate the cell membrane. Once inside the cell, esterases in the cell cleave the acetoxymethyl ester from the BCECF thus making it hydrophilic and trapping it in the cell. BCECF-AM was purchased as 1mg aliquots (Molecular Probes) and transferred into ~293µl of DMSO to form a 5mM stock solution which was stored at -20°C in a light protected container. Approximately 1 hour after preparing the brainstem slices, the BCECF-AM was thawed and vortexed. The slices were transferred to a 25ml beaker which contained 5ml of aCSF equilibrated with 95%O_2-5%CO_2 (pH ~7.45). 20µl of BCECF-AM was then added to 5ml of aCSF to yield a final loading concentration of 20µM and the slices were incubated for ~30mins in a water bath at ~37°C. After 30 mins of loading, the slices were transferred back into aCSF (room temperature). For optimal visualization, the slices were allowed to wash for at least 30 mins to allow for dye not taken up by cells to be washed away.

Dihydroethidium loading.

The dye used in the experiments that involved measuring the rate of production of reactive oxygen species (ROS) was dihydroethidium (DHE) which was purchased from Molecular Probes as a 5mM stock in DMSO. Due to the fact that DHE has a tendency to leak out of neurons, each slice was loaded individually just prior to each experiment and no wash time was allowed following loading. This protocol was different from that of BCECF where all the slices were loaded once and then allowed to wash until experiments were ready to be run. The protocol for DHE was as follows: individual slices were transferred to a 25ml beaker which contained

10ml of aCSF equilibrated with 95%O_2-5%CO_2 (pH ~7.45) and 20µl of DHE. The slice was incubated in the dye (10µM) for ~30mins at ~37°C and then following loading was placed directly into the superfusion chamber (discussed below) for visualization.

Chamber conditions

The superfusion chamber used during experiments is a 750µL Plexiglas superfusion chamber with the bottom made of a thin glass coverslip (~180µm thick). Individual slices were placed in this chamber and immobilized with a grid made of nylon fibers held on a U-shaped platinum frame. All solutions were held in 140ml syringes in a water bath (~37°C) on a shelf above the superfusion chamber. Control solution was equilibrated with 95%O_2-5%CO_2 while hypoxic solutions were equilibrated with 95%N_2-5%CO_2. Both control and hypoxic solutions were equilibrated with their respective gases for ~30 mins. Solution was flowed (gravity feed) to the chamber through stainless steel tubing (outer diameter 1.6mm, 0.5mm inner diameter), a glass bubble trap and through a thermoelectric Peltier assembly maintained at ~37°C. From this point, the solution perfused over the slice from one side at ~2-4ml/min and was removed from the alternate side via a vacuum line. The superfusion chamber was placed on the stage of an inverted Nikon Diaphot microscope in order to visualize the underneath surface of the slice. Accidental movements and vibrations were minimized by placing the entire microscope on a Micro-g (Technical Manufacturing Corp.) air table.

Visualization of BCECF-loaded slices

In order to excite the slices, light from a 75W Xenon arc lamp was passed through a 16 neutral density filter and then through either a 500 ± 10 or 440 ± 10 nm filter (25 mm diameter, Omega Optical) alternately. Both filters were held in a Lambda 10-2 (Sutter Instruments Co.) filter wheel which rotated each filter into position in 400ms. The excitation light was reflected by a Nikon DM510 dichroic mirror through a Nikon 40X Fluor Objective (N.A. 0.85) which focused the light on the region of the slice of interest. Once excited, the BCECF emitted fluorescence was collected through the 40X objective and then passed through a 530 ± 10nm emission filter (Omega Optical). The emitted fluorescence continued through a GenIIsys image intensifier (Dage-MTI, Inc.) which allowed for lower levels of excitation light by amplifying the fluorescence signal, thereby preventing photobleaching. The fluorescent light then passed through a CCD72 camera, a GenIIsys intensifier gain controller box and a CCD72 camera gain and black level controller box (all of which were purchased from Dage-MTI, Inc.). The final image was acquired by a Gateway 2000 Pentium II computer, processed with Metafluor Imaging Software (Universal Imaging) and displayed on a Sony RGB Monitor. Images were stored on the Gateway computer hardrive for later analysis (Figure 6).

Imaging of BCECF loaded slices

Once the slice had been loaded with BCECF-AM and allowed to wash for 1 hour, it was placed in the superfusion chamber and perfused with control aCSF at ~3ml/min. Using brightfield microscopy, the region of interest was identified under both 10X and then 40X objectives. Switching to fluorescence microscopy and using

the 500nm excitation wavelength, an image of the neurons on the computer was optimized by adjusting the gains, black levels and focus. A background image was taken by blocking off light to the camera and was subtracted from all subsequent images captured during the experiment. When BCECF is excited by light of 500nm, the fluorescence is maximally pH sensitive and when excited by light of 440nm, the fluorescence is nearly pH insensitive (Bright et al., 1989; Putnam and Grubbs., 1990; Ritucci et al., 1996). In order to compare pH_i to fluorescence, a ratio of Fl_{500}/Fl_{440} is determined which yields R_{fl}. R_{fl} is an indication of whether the pH_i is changing or whether the probe is undergoing photobleaching or dye leakage. Images are gathered every minute at 500 and 440nm wavelengths and an R_{fl} value is calculated. Experiments began with an initial control baseline of ~5-10mins followed by experimental conditions. During analysis, R_{fl} is converted to pH_i by means of a calibration curve derived from a high K^+/nigericin calibration technique (Ritucci et al., 1996; Thomas et al., 1979).

Imaging of DHE loaded slices

The ROS-sensitive fluorogenic probe, dihydroethidium (DHE), was used to measure the rate of production of ROS (specifically superoxide). When DHE is exposed to intracellular superoxide ($\cdot O_2^-$), it is oxidized to the fluorescent product ethidium (Eth). By monitoring the change in fluorescence intensity produced by Eth, relative superoxide levels in the cell can be measured. Ethidium is excited by a wavelength of light of ~525 ± 50nm and emits a fluorescent wavelength of 590 ± 50nm. To account for the difference between DHE and BCECF, a few minor alterations were made to the setup. Light from the 75W Xenon arc lamp is passed through a ~525nm filter

instead of the two filters of ~500 and 440nm used with BCECF. In addition, the ~530nm emission filter was replaced with a ~590nm emission filter. During the experiment, instead of taking two images at 500 and 440nm wavelengths every minute, a single image was captured at ~590nm every 3 minutes. Similarly to BCECF, the experiments began by attaining a stable fluorescence signal for ~5-10mins and this was considered the control baseline. The captured images were stored for later analysis.

Data Analysis

For BCECF: All R_{fl} values obtained from each experiment were normalized to the R_{fl} value at pH of 7.2 by dividing each R_{fl} value by the R_{fl} at a pH of 7.2 (in K^+/nigericin). This normalized R_{fl} (N_{fl}) was then converted into pH_i using the following equation $pH_i = 7.272 + \log (N_{fl} – 0.0841/1.9725 – N_{fl})$.

For DHE: An average value for the first 5 minutes of steady-state baseline was obtained and all data was normalized to this average value. Fluorescence intensity was reported as the relative change from this initial average value.

Statistics

All data are presented as the mean ± SEM. Student's paired t-tests with a level of significance of $P< 0.05$ were used for determining statistical significance between 2 means.

FIGURE 6. Schematic of the experimental arrangement used for imaging fluorescence in dye-loaded slices (Modified from Ritucci et al., 1996).

FIGURE 6.

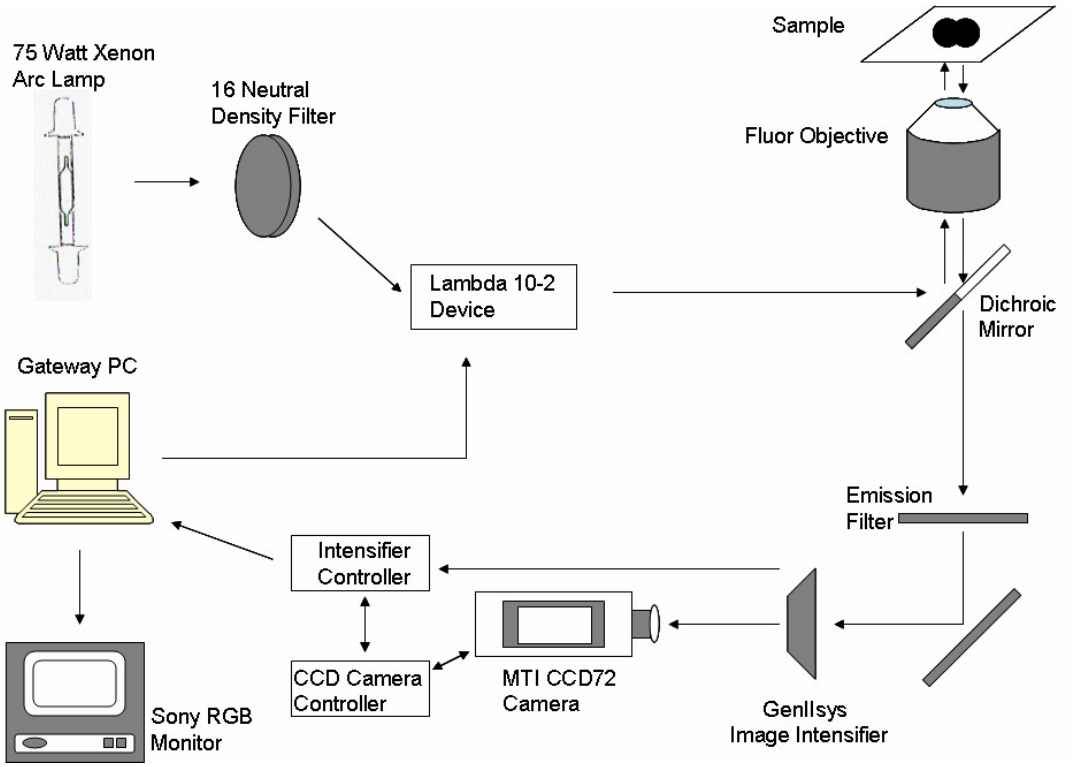
75 Watt Xenon
Arc Lamp
16 Neutral
Density Filter
Lambda 10-2
Device
Sample
Fluor Objective
Dichroic
Mirror
Gateway PC
Emission
Filter
Intensifier
Controller
CCD Camera
Controller
MTI CCD72
Camera
GenIIsys
Image Intensifier
Sony RGB
Monitor

CHAPTER V

THE RELATIONSHIP BETWEEN LACTIC ACID, REACTIVE OXYGEN SPECIES AND THE HYPOXIA-INDUCED ACIDIFICATION SEEN IN CHEMOSENSITIVE NEURONS OF THE NUCLEUS TRACTUS SOLITARIUS (NTS)

(Prepared in manuscript format for "Respiratory Physiology & Neurobiology")

1. Introduction

There are cells in our body that are able to alter the frequency and depth of breathing in response to changes in blood gas levels. These neurons are commonly known as chemoreceptors and there are both peripheral and central chemoreceptors located in different regions within our body. The central chemoreceptors were initially thought to be localized to the medulla of the brainstem, but in more recent years several regions have been identified as being chemosensitive. These regions include the nucleus tractus solitarius (NTS)(Dean et al., 1989), the medullary raphe (Richerson, 1995), locus coeruleus (Filosa et al., 2002), pre-Bötzinger complex (Solomon et al., 2000), retrotrapezoid nucleus (Guyenet et al., 2005; Mulkey et al., 2004; Ritucci et al., 2005) and neurons of the ventral medulla (Miles, 1983).

These regions are defined as chemosensitive because they contain neurons that respond to changes in CO_2/H^+, have axonal projections to a respiratory control center and can ultimately lead to a change in ventilation (Putnam et al., 2004). Only a portion of the neurons in these regions are considered chemosensitive and only two of these regions, the NTS and pre-Bötzinger complex have been shown to respond to oxygen (Pascual et al., 2002; Solomon et al., 2000). Although the single specific stimulus for these neurons has yet to be identified, the neurons respond well to both increased CO_2 (hypercapnea) and decreased intracellular pH (pH_i). Interestingly, studies have shown the neurons of the NTS to acidify in response to hypoxia (Chambers-Kersh et al., 2000) but this acidification does not appear to stimulate ventilation. This phenomenon has subsequently been referred to as the hypoxia

paradox (Nattie, 1998) because acidification of intracellular neuronal contents from hypercapnia results in an increase in neuronal firing rate but the acidification induced by hypoxia does not. Our study was directed at identifying the source of the hypoxia-induced acidification seen in neurons of the NTS. By identifying the cause of this acidification, perhaps we can begin to understand why these neurons will increase their firing rate in response to an acidification induced by hypercapnea but not one induced by hypoxia.

The most obvious answer as to why these neurons acidify in response to hypoxia is that the cells of the central nervous system will switch to anaerobic metabolism in an attempt to maintain the production of ATP in the absence of O_2. By switching to anaerobic metabolism, the neurons and glial cells will produce larger quantities of lactic acid which could be the source of the acification. A portion of this study focuses on the glial cells as the source of this lactic acid and a separate portion focuses on the neurons as the source. Two separate approaches were used to prevent the production of lactate by both neuronal and glial cells. The first involved using an oxygen-glucose deprived solution (OGD) which starved the cells of glucose, the substrate necessary to produce lactate, and the second involved using iodoacetate which blocks glycolysis. To focus specifically on the glial cells as the source of the lactate, we used two compounds which specifically target glial cells.

It has been suggested that during times of increased neuronal metabolic demand, glial cells use a large amount of their glucose supplies to produce lactate and then shuttle that lactate over to the neurons to be used as an alternative substrate to produce energy (Pellerin et al., 2004). For instance, studies have shown that

glutamate increases the breakdown of glucose and the production of lactate in glial cells (Pellerin et al., 1994). In addition to this, another study shows that glutamate increases the uptake of glucose into glial cells significantly (Loaiza et al., 2003). This movement of lactate from the glial cell to the neuron could account for the hypoxia-induced acidification seen in the neurons of the NTS. However, this lactate shuttle would not be beneficial to neurons during hypoxia due to the fact that there is no oxygen available for the neurons to use to degrade lactate to generate more energy. As previously mentioned, we used two compounds which specifically target glial cells to ensure that the lactate produced by glial cells does not account for the hypoxia-induced acidification previously mentioned. The two compounds are fluorocitrate (FC) and 4-hydroxycinnamate (4-Cinn). FC is a potent glial toxin which will essentially stop glial cell metabolism (Clarke et al., 1970) thereby preventing the production of lactate, whereas 4-Cinn specifically blocks the monocarboxylate transporters used to move lactate out of the glial cell and into the neuron (Dringen et al., 1993, McKenna et al., 2001).

With four different approaches (OGD, iodoacetate, FC and 4-Cinn) this study will try to isolate whether the hypoxia-induced acidification is due to lactic acid production and which cells, neurons or glia, are responsible for this lactic acid. In the event that lactic acid is not the source of the hypoxia-induced acidification seen in the neurons of the NTS, we suggested another mechanism for this acidification and this formed the second portion of this study. We turned to reactive oxygen species (ROS) as the second possible source of the hypoxia-induced acidification. It is a commonly held belief that during the reoxygenation portion of a hypoxic bout, levels of ROS

increase. The proposed mechanism for this is that during the reoxygenation, the cells are exposed to relative hyperoxia and hyperoxia increases the production of ROS (for review consult: Jamieson et al., 1986). From a review of the literature, it is our understanding that very few studies have actually measured the levels of ROS during a hypoxic bout but have rather measured the subsequent effects of the ROS such as oxidation of cellular proteins and lipid peroxidation. Our suggestion is that perhaps ROS increase during the hypoxic exposure itself prior to reoxygenation and that this increase in ROS accounts for a portion of the hypoxia-induced acidification seen in neurons of the NTS. This theory is based upon recent studies which have shown ROS to increase during hypoxia (Magalhaes et al., 2005; Becker et al., 1999). One suggested mechanism as to how ROS increase during hypoxia is that hypoxia blocks cytochrome complex III of the mitochondrial electron transport chain which then causes this protein to produce large quantities of superoxide (Chandel et al., 2000). It is therefore not unheard of for ROS to increase during hypoxia.

As a result, we directed the second half of this study to measuring ROS in neurons of the NTS during hypoxia and then correlating this change in ROS to the hypoxia-induced acidification. Our lab has shown that chemical oxidants and ROS generating compounds are able to acidify neurons of the NTS (Mulkey et al., 2004). Other studies with hydrogen peroxide have shown an acidification in a variety of cells (Tsai et al., 1997; Chao et al., 2002). There are many suggested mechanisms as to how ROS causes an intracellular acidification. It has been suggested that oxidative stress causes oxidation of cysteine and methionine residues of the Na^+/H^+ exchanger which renders it unable to control intracellular pH (Mulkey et al., 2004, Hu et al.,

1998). Another possibility of ROS causing a decrease in pH_i could involve ROS blocking oxidative phosphorylation. There is some evidence that oxidative stress increases lactic acid production in the CNS (Chan et al., 1982) and this could potentially be due to ROS blocking oxidative phosphorylation (Chance and Boveris, 1978). Mulkey and others have also suggested that hydrogen peroxide and oxidative stress increases the hydrolysis of ATP which leads to an increase in cytosolic hydrogen concentration.

To begin this ROS portion of the study, we initially measured ROS with a superoxide specific probe dihydroethidium (DHE). We then used ROS scavenging compounds melatonin (an antioxidant) and MnTMPyP (a superoxide dismutase mimetic) in an attempt to block the changes in ROS that we observed during hypoxia. Finally, we reverted back to measuring pH_i during hypoxia and used the aforementioned ROS scavengers to monitor their effects on the hypoxia-induced acidification.

2. Methods

2.1 Slice preparation

Protocols for preparing both NTS and RTN brainstem slices have been previously described (Ritucci et al., 1996, Ritucci et al,. 2005). Briefly, the brainstem from a Sprague-Dawley rat pup ranging in postnatal age from P1-P12 days was isolated. Slices were taken from both medullary and pontine regions to yield both NTS and RTN respectively. For NTS, slicing began at the obex and moving rostrally ~900μm, transverse medullary brain slices (200-300μm) were cut using the Vibratome(series 1000) sectioning system. For RTN, transverse pontine slices (200-

300μm) were taken beginning caudal to cranial nerve VII and slicing for ~900μm. Slices were incubated at room temperature in aCSF equilibrated with 95% O_2-5% CO_2 (control, pH ~ 7.45) and allowed to recover for at least 30mins. All procedures involving the use of animals were in agreement with the Wright State University Animal Care and Use Committee guidelines and were approved by the committee. Wright State University is accredited by the AAALAC and is covered by NIH Assurance (no. A3632-01).

2.2 Solutions

Control solution contained (in mM) 124 NaCl, 5.0 KCl, 1.24 NaH_2PO_4, 1.3 $MgSO_4$, 2.4 $CaCl_2$, 26 $NaHCO_3$, and 10 glucose and was equilibrated with 95% O_2-5% CO_2 (control, pH ~ 7.45 at 37° C). Hypoxic solution used in certain experiments was standard aCSF equilibrated with 95%N_2-5%CO_2 (pH ~7.45 at 37° C). Experiments that involved starving the cells of both oxygen and glucose employed an oxygen-glucose deprived solution (OGD) in which, 10mM glucose was replaced isoosmotically with 10 mM 2-deoxy-$_D$-glucose and equilibrated with 95%N_2-5%CO_2. Two separate compounds were used in the studies of the role of glial cells in the hypoxia-induced acidification. The first was the glial toxin fluorocitrate (FC; Sigma-Aldrich) which works by inhibiting aconitase, the enzyme critical for the conversion of citrate to isocitrate in the tricarboxylic acid cycle (1mM). The second compound used was 4-hydroxycinnamate (4-Cinn; Sigma-Aldrich) which is an inhibitor of the monocarboxylate transporters (MCT) found on both neurons and glial cells. MCT1, the monocarboxylate transporter found on glial cells is inhibited by 4-Cinn at a concentration of ~500μM, whereas MCT2 found on neurons is inhibited at a

concentration of ~25μM. We used a concentration of 500μM to inhibit both MCT1 and MCT2. Iodoacetate was used to block metabolism of both neuronal and glial cells by blocking the enzyme glyceraldehyde-3-phosphate dehydrogenase (GAPD). Iodoacetate was purchased from Sigma Aldrich as sodium iodoacetate and added to aCSF to yield a final concentration of 5μM. Two compounds, melatonin (Mel; 100μM) and manganese(III)tetrakis(1-methyl-pyridy)porphyrin pentachloride (MnTMPyP; 25μM) were used to scavenge ROS and were prepared by adding them directly to standard aCSF which was equilibrated with 95%O_2-5%CO_2 (control, pH ~ 7.45 at 37° C). In those experiments that involved both mel and MnTMPyp, the compounds were both added to standard aCSF at concentrations of 100μM and 25μM, respectively.

2.3 Chamber conditions

The superfusion chamber used during experiments was a 750μL Plexiglas superfusion chamber with the bottom made of a thin glass coverslip (~180μm thick). Individual slices were placed in this chamber and immobilized with a grid made of nylon fibers held on a U-shaped platinum frame. All solutions were held in 140ml syringes in a water bath (~40°C) on a shelf above the superfusion chamber. Control solution was equilibrated with 95%O_2-5%CO_2 while hypoxic solutions were equilibrated with 95%N_2-5%CO_2. Solution was flowed (gravity feed) to the chamber through stainless steel tubing (outer diameter 1.6mm, 0.5mm inner diameter), a glass bubble trap and through a thermoelectric Peltier assembly maintained at ~37°C. From this point, the solution perfused over the slice from one side at ~2-4ml/min and was removed from the alternate side via a vacuum line. The superfusion chamber was

placed on the stage of an inverted Nikon Diaphot microscope in order to visualize the underneath surface of the slice. Accidental movements and vibrations were minimized by placing the entire microscope on a Micro-g (Technical Manufacturing Corp.) air table.

2.4 BCECF loading and imaging of slices

Slices were allowed to recover for 30 mins in aCSF equilibrated with 95% O_2-5% CO_2 after slicing for 30 mins. In order to measure pH_i, the slices were loaded with 20 μM BCECF-AM for 30 mins at 37° C and washed at room temperature for 30 mins following loading. Individual slices were placed in the superfusion chamber mentioned above and perfused with aCSF heated to 37° C (pH ~ 7.45) at 2ml/min. The dye was excited every 60s by alternating pulses of light (from a xenon arc lamp) with wavelengths of 500nm (pH sensitive) and 440nm (pH insensitive) with a Sutter Lambda 10-2 filter wheel (all filters were from Omega Optical). The emitted fluorescence was directed through a 530 ± 10nm emission filter (Omega Optical) and continued through a GenIIsys image intensifier, CCD72 camera, a GenIIsys intensifier gain controller box and a CCD72 camera gain and black level controller box (all of which were purchased from Dage-MTI, Inc.). The final image was acquired by a Gateway 2000 Pentium II computer, processed with Metafluor Imaging Software (Universal Imaging) and displayed on a Sony RGB Monitor. Images are stored on the Gateway computer hardrive for later analysis.

pH_i is proportional to the ratio of emitted fluorescence (530 nm) at the two excitation wavelengths of 500nm and 440nm. Images were collected and processed using Metafluor Imaging software. Fluorescence ratios were then converted to pH_i by

means of a calibration curve derived from a high K^+/nigericin technique (Ritucci et al., 1997; Thomas et al., 1979).

2.5 Dihydroethidium loading and imaging.

The dye used in the experiments that involved measuring the quantity of reactive oxygen species (ROS) was dihydroethidium (DHE). The DHE was purchased from Molecular Probes as a 5mM stock in DMSO and a final concentration of 10μM was used during loading. Individual slices were loaded in freshly made dye just prior to each experiment and slices were loaded at 37° C for ~30mins. Slices were then transferred to the superfusion chamber previously mentioned. Relative superoxide levels were measured by monitoring the increase in Ethidium (Et) fluorescence which is generated by the oxidation of DHE by intracellular $\cdot O_2^-$. The Et fluorescent product was excited by a wavelength of light of 525nm and the emitted fluorescence of 590nm was collected and processed using Metaflour Software (Universal Imaging). Measurements of fluorescence intensity were taken every 3 minutes to limit phototoxicity and photobleaching. In both pH_i and ROS experiments, standard protocols were as follows: An initial control period of ~5-10mins was observed which involved ensuring that a stable fluorescence signal could be maintained in standard aCSF. Slices were then exposed to a 10 minute bout of hypoxia followed by another control period of 10 minutes to allow for recovery. The drug of interest was then applied for at least 20 minutes, in some cases longer depending on the mechanics of the compound, and then a second hypoxic bout of 10 minutes in the presence of the drug was applied. The slice was then allowed a final recovery from insult.

2.6 Data collection and analysis.

All data were collected using the Metaflour imaging software (Universal Imaging). pH_i was proportional to the ratio of fluorescence (R_{fl}) intensity. Fluorescence intensity was normalized (N_{fl}) to the R_{fl} value at pH 7.2 and converted to pH_i using the following equation $pH_i = 7.272 + \log (N_{fl} – 0.0841/1.9725 – N_{fl})$. With regards to the DHE experiments, data were normalized to the average fluorescence intensity during the first 10 minutes of baseline. Values were reported as a change in absolute fluorescence units (AFU) from the normalized fluorescence intensity.

2.7 Statistical Analysis.

All data are presented as the mean ± SEM. Student's paired t-tests and 1 sample t-tests with a level of significance of $P<0.05$ were used for determining statistical significance.

3. Results

3.1 Effects of hypoxia on pH_i.

Using the pH fluorescent probe BCECF, measurements of neuronal pH_i were made during hypoxia and compared to measurements of pH_i during hypoxia and an experimental drug. From a total of 473 neurons, the mean pH_i change under hypoxic conditions was 0.13±0.002 pH units (Figure 7). The 473 neurons were in 48 different brainstem slices from 33 different rats. Throughout the paper, n is reported as the number of neurons which were monitored per experimental series.

3.2 Oxygen-glucose deprivation (OGD)

Experiments were run comparing the ΔpH_i during hypoxia versus oxygen glucose deprivation (OGD). The rationale for these experiments was to determine whether removing glucose would remove the substrate necessary for both the neurons and the glial cells to produce lactic acid. If lactic acid is responsible for the hypoxia-induced acidification, we should see a reduction in the magnitude of the acidification when we administer OGD. The brainstem slice was exposed to 10 minutes of hypoxia, which was used as a control response OGD, and then exposed to 10 minutes of OGD. The order of exposure was randomized in a few experiments to ensure that the change in pH_i was not dependent on neuronal injury and dysfunction after repeated bouts of hypoxia. The ΔpH_i during these experiments under hypoxic conditions was 0.12±0.002 pH units whereas under OGD conditions mean ΔpH_i was 0.10±0.002 pH units (n=140). Although the difference in pH_i between these two conditions of O_2 deprivation for the population sampled is likely not to be considered physiologically relevant, a group of 56 neurons in the NTS did show a significant blunting of pH_i of more than 25% or 0.03 pH units (Figure 8).

3.3 Iodoacetate vs. hypoxia

The pH_i response of NTS neurons to hypoxia was further studied using iodoacetate, an inhibitor of glycolysis. The primary intent with these experiments was to block glycolysis in both neurons and glial cells and in doing so, we would prevent the production of lactic acid. Assuming that the hypoxia-induced acidification was due to lactic acid, we should then see a reduction in the acidification during hypoxia.

FIGURE 7. Indicates a pH_i trace in a single neuron from the nucleus tractus solitarius (NTS) exposed to 2 bouts of hypoxic solution (aCSF equilibrated with 95%N_2-5%CO_2). Hypoxic exposures were approx. 10 minutes in length and images were taken every minute. The mean baseline pH_i was calculated just prior to the hypoxic incident and then recalculated around the lowest pH point during the exposure. Subtracting the mean pH_i during a hypoxic incident from the mean baseline pH_i yielded the overall acidification, or delta pH_i. Mean delta pH_i was 0.13±0.002 (n=473).

FIGURE 7.

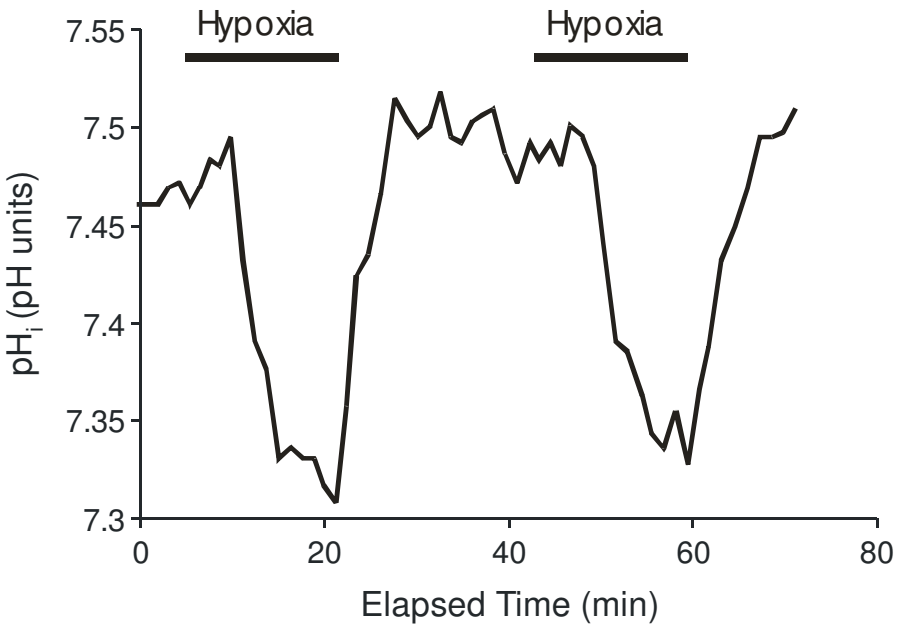
Hypoxia
Hypoxia
7.55
7.5
7.45
7.4
7.35
7.3
pH$_i$ (pH units)
0
20
40
60
80
Elapsed Time (min)

FIGURE 8 . Two pH_i traces taken from two separate neurons of the NTS are shown. The grey or lighter colored trace represents the general trend seen in these neurons following a 10 minute exposure to hypoxia and a 10 minute exposure to OGD. The mean ΔpH_i during these experiments under hypoxic conditions was 0.12±0.002 pH units whereas under OGD conditions mean ΔpH_i was 0.1±0.002 pH units (n=140). The black or darker colored trace represents a group of 56 neurons that experienced a significant blunting of the acidification (decrease of ~25%) under OGD conditions.

FIGURE 8.

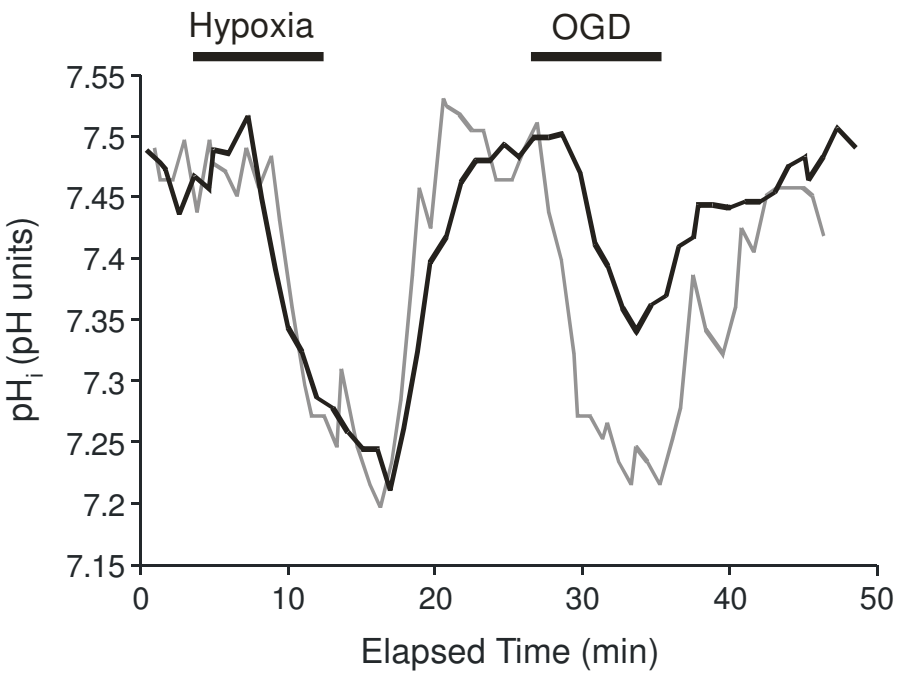
Hypoxia
OGD
7.55
7.5
7.45
7.4
7.35
7.3
7.25
7.2
7.15
pH$_i$ (pH units)
0
10
20
30
40
50
Elapsed Time (min)

The slice was initially exposed to 10 minutes of hypoxia followed by a recovery period. The iodoacetate was then applied for ~20-30 minutes followed by a 10 min bout of hypoxia under iodoacetate conditions. Mean ΔpH was 0.18±0.007 under hypoxic conditions and 0.08±0.005 under iodoacetate and hypoxic conditions (n=39) (Figure 9). The blunting of the pH_i response under iodoacetate (decreased by 53%) and hypoxic conditions was statistically significant ($p<0.001$).

3.4 Fluorocitrate studies

Fluorocitrate has been established as a potent glial toxin because it inhibits the enzyme aconitase which is needed for the tricarboxylic acid cycle to convert citrate into isocitrate. Thus, we predicted that if we exposed the slice to fluorocitrate we would prevent the glial cell metabolism and thus reduce the flux of lactic acid from the glial cells to the neurons. We then therefore expect the hypoxia-induced acidification to be blunted as a result. We would also expect that once the glial cells are compromised, they would be unable to maintain extracellular pH in which case, the neuronal pH should acidify during exposure to the FC alone, which has been previously shown by Erlichman and others (Erlichman et al., 1998). During these experiments, the brainstem slice was exposed to an initial 10 minute bout of hypoxia followed by a recovery period. The slice was then exposed to FC for ~30mins and then FC in conjunction with hypoxia for 10mins. These experiments were performed in both the NTS and the RTN due to the fact that recent studies suggest that the NTS does not contain a significant quantity of glial cells during this range of postnatal ages (Erlichman et al., 2004). The RTN, on the other hand, is known to have high amounts of glial cells over this range of postnatal age (Erlichman et al., 2004).

FIGURE 9. pH_i trace represents a single NTS neuron exposed to hypoxia followed by application of iodoacetate and re-exposure to hypoxia under iodoacetate conditions. Iodoacetate is subsequently removed and approx. 20 mins of washout time is allotted. Neuron is then re-exposed to hypoxia in the absence of iodoacetate. As the trace indicates, the acidification under iodoacetate is blunted significantly. Mean delta pH_i under hypoxic conditions was approx. 0.18±0.007 and under iodoacetate and hypoxic conditions was 0.08±0.005 (n=39).

FIGURE 9.

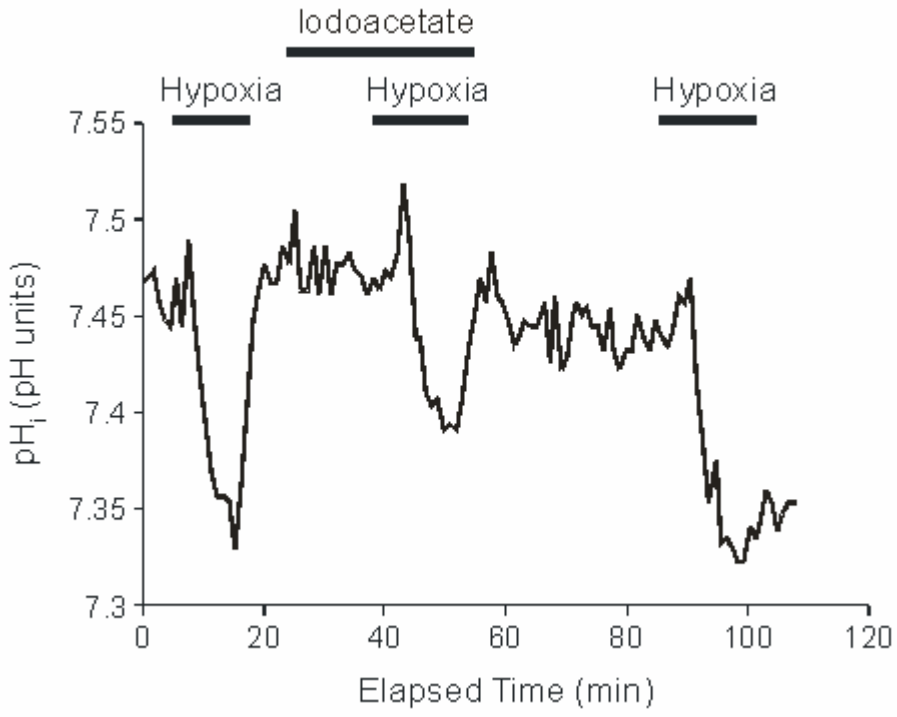
Iodoacetate
Hypoxia
Hypoxia
Hypoxia
7.55
7.5
7.45
7.4
7.35
7.3
pH$_i$ (pH units)
0
20
40
60
80
100
120
Elapsed Time (min)

Experiments run in the RTN had a mean pH_i change under hypoxic conditions of 0.10±0.003 pH units. The delta pH_i during fluorocitrate and hypoxic conditions was approximately 0.09±0.003 pH units (n=66). Figure 10 illustrates that neurons of the RTN experienced an acidification under FC conditions alone. Conversely, we were unable to produce the same acidification in neurons of the NTS. This suggests that at this particular age the RTN contains a significantly larger quantity of glial cells than that of NTS, whereas the NTS is relatively deficient of glial cells

NTS experiments run with FC experienced a mean pH_i change of 0.11±0.007 under hypoxic conditions and a mean pH_i change of 0.10±0.008 under fluorocitrate conditions and hypoxia (n=24). Experiments in the NTS did not show an acidification under standard FC conditions like those of the RTN (Figure 10).

3.5 4-Cinnamate effects

4-hydroxycinnamic acid (4-Cinn) has been shown to be a selective blocker of the MCT1 and MCT2 transporters found on neurons and glial cells (Dringen et al., 1993; McKenna et al., 2001). Thus, the response to hypoxia was studied in both neurons from RTN and NTS, in absence and presence of 4-Cinn, to establish whether there was an effect of 4-Cinn on the hypoxia-induced acidification. If so, this would suggest that the neuronal acidification was due to lactic acid produced by the glial cells and shuttled over to the neurons in conjunction with hydrogen ions.

pH_i measurements were made in the RTN and NTS brain slices. The slices were exposed to 10 minutes of hypoxia, followed by 10 minutes of control to allow the neurons to recover to baseline pH. The slices were then exposed to 4-Cinn for

FIGURE 10. Indicates pH_i traces of single individual neurons in the NTS and RTN during exposure to FC. The RTN neuron is represented by the black trace whereas the NTS is represented by the grey trace. As the figure illustrates, an acidification of baseline pH_i occurred in the RTN neuron but not the NTS neuron. Regardless of this fact, neither NTS nor RTN neurons exhibited a significant change in the acidification during hypoxia compared to that of hypoxia and FC. Delta pH_i for RTN during hypoxia was 0.10±0.003 and during experimental conditions was 0.09±0.003 (n=66). Delta pH_i for NTS neurons was 0.11±0.007 and 0.10±0.008 (n=24).

FIGURE 10.

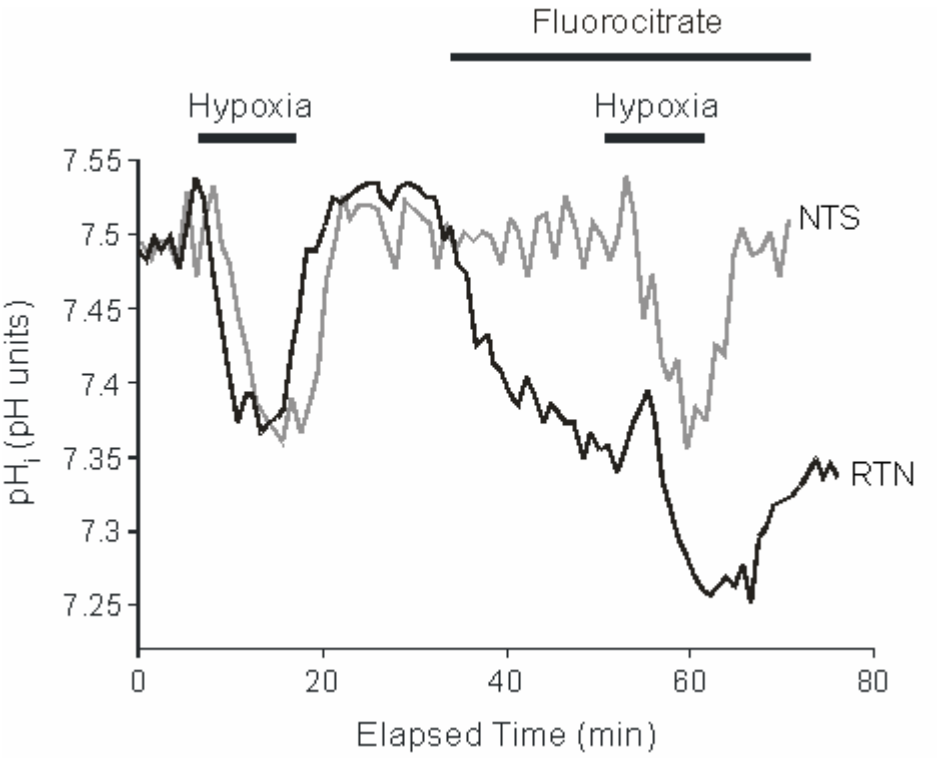
Fluorocitrate
Hypoxia
Hypoxia
NTS
RTN
7.55
7.5
7.45
7.4
7.35
7.3
7.25
pH$_i$ (pH units)
0
20
40
60
80
Elapsed Time (min)

approximately 30 minutes and under these conditions were then exposed to hypoxia for a second 10 minute bout.

There was no acidification of baseline pH in NTS cells under 4-Cinn conditions. Likewise, the mean ΔpH_i during hypoxia was 0.15±0.008 and under 4-Cinn and hypoxia ΔpH_i was 0.17±0.01 (n=80). Based upon these results, there was not a significant blunting of pH_i during hypoxia plus 4-Cinn compared to that of hypoxia alone (Figure 11). Thus, these experiments were repeated in the RTN, which gave similar results. 4-Cinn did not alter baseline pH under control conditions. In addition, 4-Cinn did not change the pH response to hypoxia. Mean ΔpH_i during hypoxia was 0.12±0.003 and under 4-Cinn and hypoxia was 0.11±0.004 (n=86).

3.6 Relative changes in ROS under hypoxic conditions

It is generally assumed that during a hypoxic incident, it is the reoxygenation portion of the bout that causes an increase in ROS. However, a large number of studies supporting this notion are based upon measuring the effects of ROS on cells, such as protein oxidation, as opposed to measuring the ROS itself. We propose in this study that ROS actually increase during hypoxia itself, not during reoxygenation. In fact, a few studies have shown ROS to increase during the hypoxic bout itself prior to reoxygenation (Magalhaes et al., 2005; Becker et al., 1999) and we propose that perhaps this increase in ROS can account for a portion of the hypoxia-induced acidification. Subsequently, using the superoxide specific fluorescent probe DHE, measurements of ROS were taken from neurons of the NTS.

FIGURE 11. pH_i traces from two separate individual neurons from the NTS and RTN exposed to 4-Cinn. RTN neuron pH_i is represented by the black trace whereas NTS is represented by the grey trace. Neither region of the brainstem experienced a difference in the acidification under hypoxic conditions versus the experimental condition. Delta pH_i during hypoxia in the RTN was 0.12±0.003 whereas with 4-Cinn and hypoxia, delta pH_i was 0.11±0.004 (n=86). In the NTS, delta pH_i under hypoxic conditions was 0.15±0.008 and under 4-Cinn conditions was 0.17±01 (n=80).

FIGURE 11.

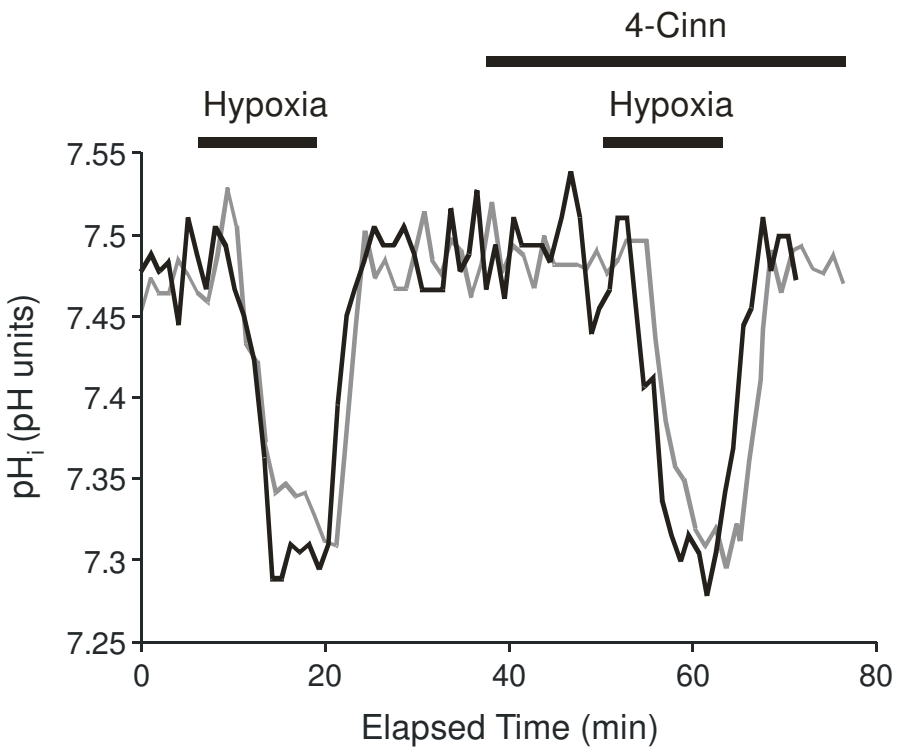
4-Cinn
Hypoxia
Hypoxia
7.55
7.5
7.45
7.4
7.35
7.3
7.25
pH$_i$ (pH units)
0
20
40
60
80
Elapsed Time (min)

The protocol for these experiments involved exposing the NTS slices to repetitive bouts of 10 minutes of hypoxia. We found that the fluorescence intensity representing changes in ROS increased during hypoxia as opposed to during re-oxygenation (Figure 12). During the post-hypoxia period, DHE fluorescence recovered, which was attributed more to the dynamics of the probe and limitations in its use rather than the time course of change in superoxide level (see Discussion). The mean increase in ROS was 12.9±0.7 absolute fluorescence units (afu) during each bout of hypoxia (n=56).

3.7 Effects of ROS scavengers – Melatonin and MnTMPyP

Studies were performed to determine whether the increase in ROS seen under hypoxic conditions could be altered with ROS scavengers melatonin and MnTMPyP. The rationale for these studies was that if we are able to blunt the increase in ROS then perhaps we could use these ROS scavengers to blunt the hypoxia-induced acidification. Subsequently, an initial bout of hypoxia was applied for approx. 10 minutes and then followed by a control period. Melatonin was applied for 10 minutes and then hypoxia in the presence of melatonin (Figure 13). The mean increase in ROS fluorescence intensity under hypoxic conditions was 12.8±0.73afu whereas under melatonin and hypoxic conditions, the mean increase was 8.6±0.56afu (n=39). Using the superoxide dismutase mimetic MnTMPyP, the mean increase in ROS under hypoxic conditions was 16.7±1.15afu whereas with MnTMPyP and hypoxia, the increase in ROS was 12.4±1.15afu (n=41) (Figure 14). Both ROS scavengers significantly blunted the production of ROS in response to hypoxia by ~25-30% ($p<0.05$).

FIGURE 12. A trace representing the relative levels of intracellular superoxide of a single neuron in the NTS during repetitive hypoxic bouts. The mean increase in ROS was 12.9±0.7afu during each bout of hypoxia (n=56). The neuron indicated in this figure shows an increase in ROS greater than that of the population mean.

FIGURE 12.

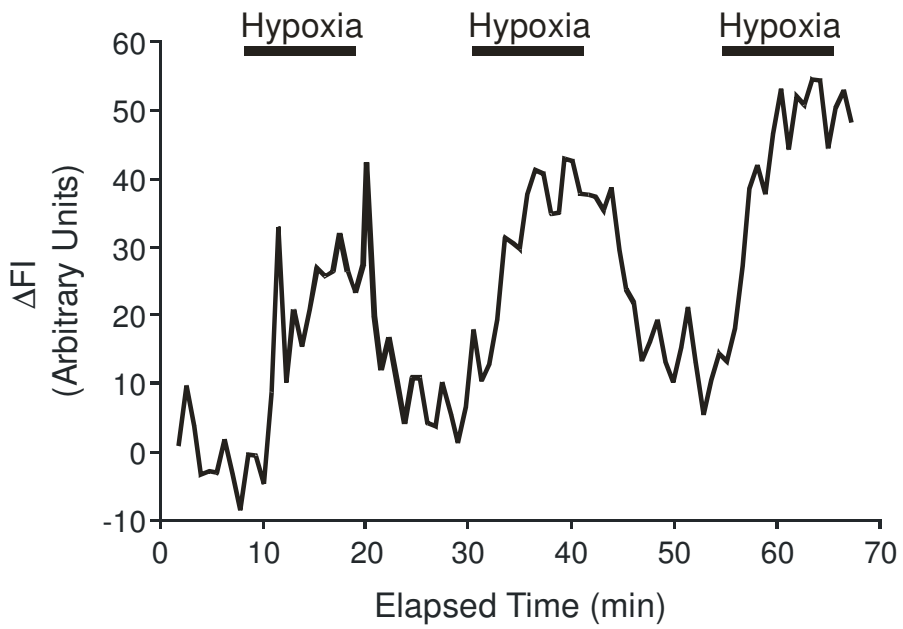
Hypoxia
Hypoxia
Hypoxia
60
50
40
30
20
10
0
-10
ΔFI
(Arbitrary Units)
0
10
20
30
40
50
60
70
Elapsed Time (min)

FIGURE 13. Trace representing the relative levels of ROS in a single neuron of the NTS. Neuron was exposed to 10 minutes of hypoxia and mean delta increase in ROS was 12.8±0.73. Melatonin was then applied and the neuron re-exposed to hypoxia in conjunction with melatonin whereby mean delta increase in ROS was 8.6±0.56 which represented a significant blunting of the response to hypoxia (n=39). The neuron indicated shows an increase in ROS greater than that of the population mean.

FIGURE 13.

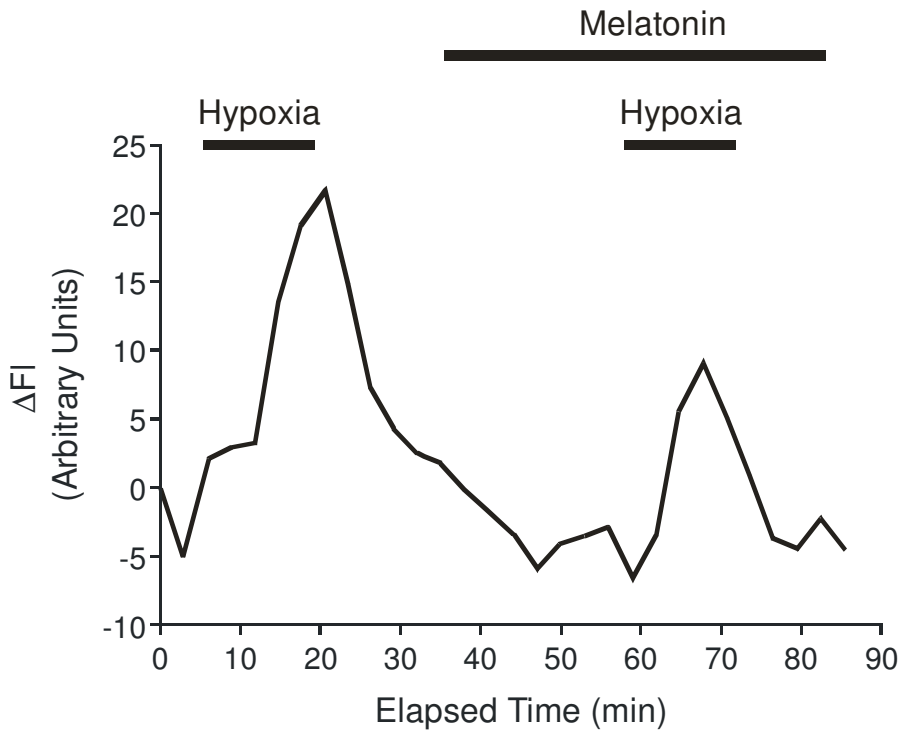
Melatonin
Hypoxia
Hypoxia
25
20
15
10
5
0
-5
-10
ΔFl
(Arbitrary Units)
0
10
20
30
40
50
60
70
80
90
Elapsed Time (min)

FIGURE 14. Trace representing the relative levels of ROS in a single neuron of the NTS. Neuron was exposed to 10 minutes of hypoxia followed by 10 minutes of control. Superoxide mimetic MnTMPyP was then applied and the neuron was re-exposed to hypoxia under these conditions. Mean increase in ROS during hypoxia was 16.7±1.15 whereas under MnTMPyP, mean increase in ROS was 12.4±1.15 indicating a significant decrease in ROS under MnTMPyP conditions (n=41). The neuron indicated shows an increase in ROS greater than that of the population mean.

FIGURE 14.

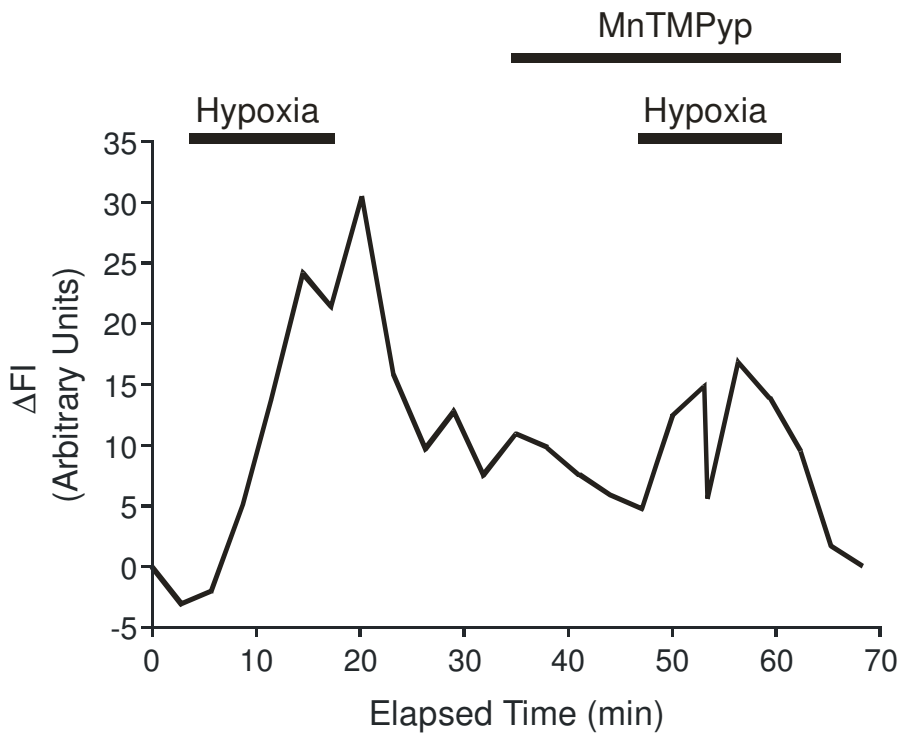
MnTMPyp
Hypoxia
Hypoxia
35
30
25
20
15
10
5
0
-5
ΔFl
(Arbitrary Units)
0
10
20
30
40
50
60
70
Elapsed Time (min)

3.8 pH_i response with Melatonin and MnTMPyP cocktail

Having established that ROS increases during a hypoxic bout and pH_i acidifies during the same exposure, studies relating the effects of a cocktail of MnTMPyP and melatonin to the acidification induced by hypoxia were performed. The cocktail of melatonin and MnTMPyP reduced the acidification by a significant amount with mean ΔpH_i during hypoxia being 0.15±0.007 and under cocktail conditions, 0.12±0.001 ($p<0.05$, $n=54$) (Figure 15).

A summary histogram of all the pH_i responses has been compiled and is indicated in Figure 16. The histogram shows the difference between the pH response during control hypoxic exposure compared to the pH response during a hypoxic exposure in conjunction with several different drug compounds.

4. Discussion

It has previously been shown that hypoxia induces an acidification in chemosensitive neurons of the NTS (Chambers-Kersh et al., 2000). During our study, we showed that this acidification was repeatable and the acidification with each hypoxic exposure was the same magnitude (Figure 7). The magnitude of the hypoxia-induced acidification in this study was within the same range of that seen in the Chambers-Kersh study previously mentioned. The magnitude was approximately 0.13pH units whereas that of the Chambers-Kersh study was between 0.1-0.3pH units. In addition, this study also showed that neurons of the RTN will acidify during a hypoxic incident which, to our knowledge, is the first time that this has been done. The RTN is of interest to us because the neurons of the RTN are chemosensitive like those of the NTS (Ritucci et al., 2005; Connelly et al., 1990; Li and Nattie, 1997).

FIGURE 15. pH_i trace of a single representative NTS neuron. During 10 minutes of hypoxia, the neuron acidified approx. 0.15±0.007. The neuron was allowed to recover to baseline whereby a cocktail of melatonin and MnTMPyP was applied. Mean delta pH_i during hypoxia in conjunction with the cocktail was 0.12±0.001 which indicated a significant decrease in pH_i (n=54).

FIGURE 15.

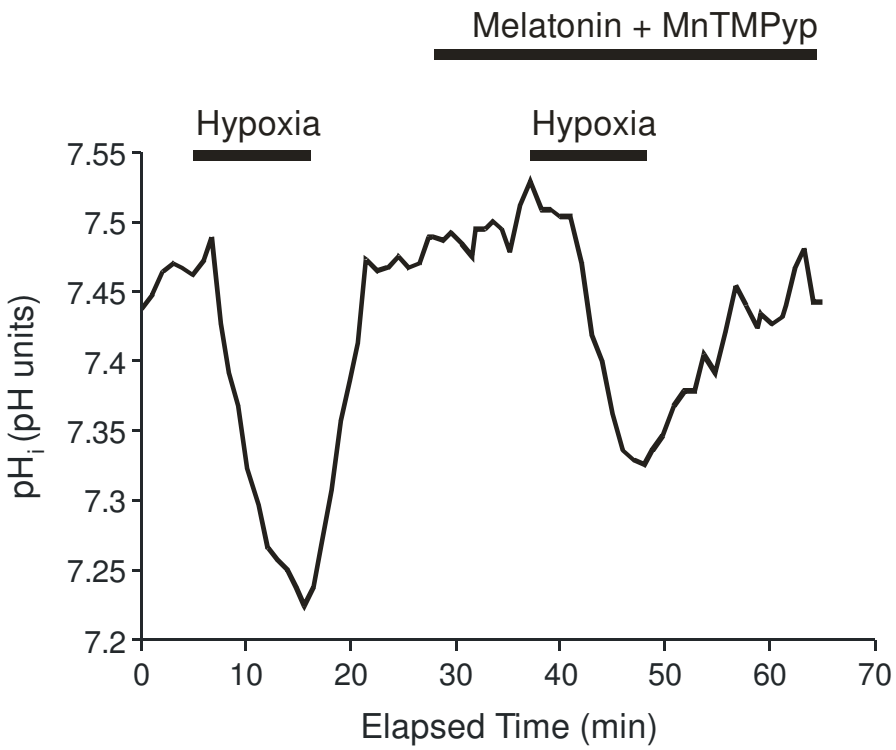
Melatonin + MnTMPyp
Hypoxia
Hypoxia
7.55
7.5
7.45
7.4
7.35
7.3
7.25
7.2
pH$_i$ (pH units)
0
10
20
30
40
50
60
70
Elapsed Time (min)

FIGURE 16. A composite histogram comparing the difference in pH_i response during hypoxia versus hypoxia in conjunction with several drugs. Bars below the zero line indicate an acidification of greater magnitude during hypoxia in conjunction with drug whereas bars above the line indicate acidification of lesser magnitude during hypoxia in conjunction with drug. The inset trace indicates that the values plotted on the Y axis are the difference between the two exposures. ** Indicates a significant difference in pH response ($p<0.05$) whereas *** indicates a highly significant difference in pH response ($p<0.001$).

FIGURE 16.

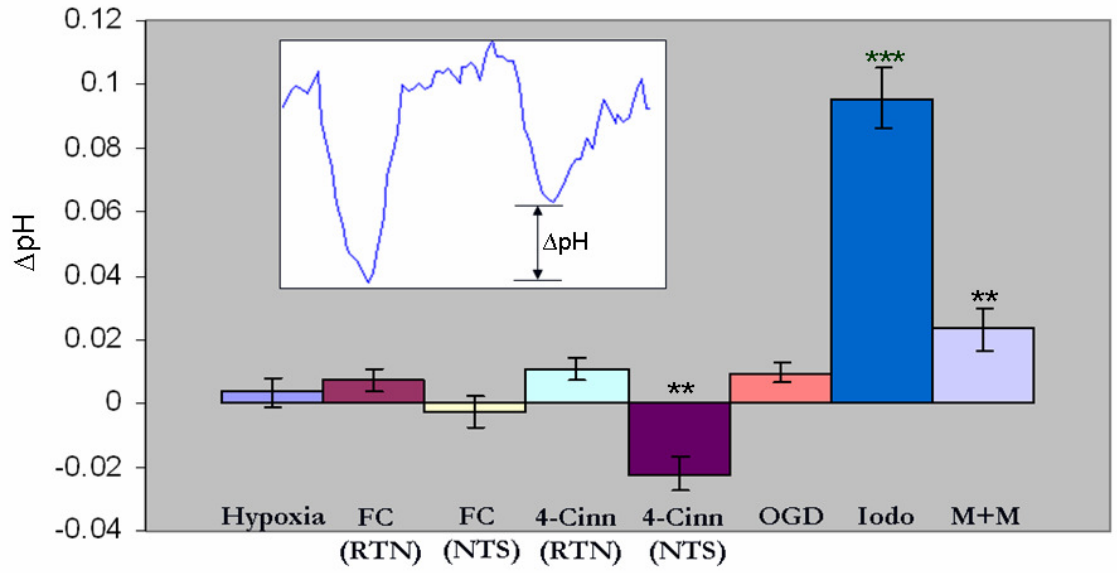
0.12
0.1
0.08
0.06
0.04
0.02
0
-0.02
-0.04
ΔpH
ΔpH
***
**
**
Hypoxia
FC (RTN)
FC (NTS)
4-Cinn (RTN)
4-Cinn (NTS)
OGD
Iodo
M+M

The hypoxia-induced acidifications in these regions are assumed to be due to increased lactic acid production during anaerobic metabolism. The purpose of this study was to isolate the cause of these acidifications and attempt to ablate the response.

4.1 Oxygen-Glucose Deprivation (OGD)

The initial thrust of the project was to focus on the relationship between the production of lactate and the hypoxic acidification. We did not specifically isolate glial cells or neurons as the source but merely focused on lactate in general. Subsequently, the first set of experiments involved oxygen-glucose deprivation (OGD) whereby we replaced glucose in standard aCSF with 2-deoxyglucose, a substrate which cells cannot use for glycolysis. In doing so, we removed the substrate required for any cells to produce lactate in which case, we expect to see a reduction in the acidification produced during OGD. Results from the experiments indicate that in a select group of cells (n=56), OGD was able to reduce the acidification significantly. As a whole population however, we did not see a significant change in the acidification during OGD conditions (Figure 8). It is not unheard of that only a small population of neurons or cells tested respond to an experimental condition. Not surprisingly though, the only finding that was consistent throughout the neurons studied was that the recovery rate from the hypoxia induced acidification was significantly slower under OGD compared to that of hypoxia. We postulate from our findings that perhaps the neurons and glial cells have adequate intracellular stores of glucose to sustain them for the relatively short 10 minute bout of OGD. The reduced rate of recovery following the OGD induced acidification can be attributed to a more

significant lack of ATP preventing the neuron from maintaining Na^+/H^+ exchange to extrude the acid.

4.2 Effects of iodoacetate

As a result of these OGD findings, the next logical approach involved the use of the compound iodoacetate (IA). Numerous studies have used IA to block metabolism in various regions of the brain (Izumi et al., 1997, Muller et al., 2003). IA works by inhibiting the enzyme glyceraldehyde-3-phosphate dehydrogenase which is a critical enzyme for glycolysis (Even et al., 1999). By using IA, we were attempting to block glycolysis and subsequently reduce the production of lactate. These experiments yielded the most promising results of the study. Observing the population as a whole, IA significantly reduced the acidification induced by hypoxia by ~50% (Figure 9). A small caveat to this approach was that in most cases, it was difficult to produce a recovery in the neurons following exposure to IA and hypoxia due to the fact that IA essentially blocks the cells ability to produce ATP altogether. In a few cases, the neurons recovered from the acidification and were subsequently allowed to wash for approx. 20 minutes. The neurons were then re-exposed to hypoxia in which case, the acidification seen during hypoxia was greater in magnitude than during IA but equal in magnitude to the initial control hypoxic exposure.

These experiments suggest to us that the primary contributing factor to the hypoxia induced acidification is lactate produced by either neurons or glial cells. Using IA, we were able to block this production of lactate and subsequently reduce the response. Due to the fact that these experiments do not isolate the neurons or glial

cells as the source of the acidification, the next thrust of the project was to focus on the glial cells as the source of the lactate.

4.3 The Impact of the Glial Cells

The next direction of the project was to focus on the relationship between the glial cells and the neuronal acidification. A variety of experiments were performed to rule out the glial cells as the source of the acidification. Current research seems to be heavily focused on the concept of an astrocyte-neuron lactate shuttle which encompasses the idea that during heightened neuronal metabolism or activity, glial cells shuttle lactate to neurons to supply them with additional metabolic substrate (for review, see Pellerin and Magistretti, 2004). The transporters that move this lactate are the monocarboxylate transporters MCT1 and MCT2 which effectively co-transport lactate in conjunction with protons. The MCT1 transporter has been localized on astrocytes whereas the MCT2 transporter has been localized to neurons (Pierre et al., 2000).

Although some research is focused on this astrocyte-neuron shuttle, we do not believe that the glial cells are the source of the lactate during a hypoxia-induced acidification. Our reason for stating this is because lactate would be of no use to a neuron without oxygen. In fact, the lactate would more than likely be detrimental for the neuron because the purpose of producing lactate during anaerobic metabolism is to generate a small amount of ATP from glucose. If lactate was shuttled from the glial cell to the neuron, this would prevent the neuron from producing it's own lactate, in which case the neuron would not be able to produce ATP in the process. It would

seem more likely that the neuron would produce it's own lactate and presumably block the uptake of lactate from the glial cell.

Additionally, lactate is shuttled from the glia to the neurons due to heightened metabolic activity of the neurons. The suggestion is that the lactate provides an additional metabolic substrate for the neuron to account for this increase in activity. However, it is well known that hypoxia causes depression of the CNS and neurons become quiescent (Kiluk et al., 2002; Ballanyi, 2004). This should reduce the flux of lactate from the glial cell to the neuron which would exclude the glia as the source of the lactate causing the hypoxia-induced acidification. Our findings during study of the glial cells as the source of lactate support this theory.

The approach for testing this aforementioned theory involved using two drug compounds. The first drug used was fluorocitrate (FC) and the second was 4-hydroxycinnamate (4-Cinn). FC has long been known to be a potent glial toxin and works by inhibiting the enzyme aconitase which catalyzes the conversion of citrate to isocitrate in the krebs cycle (Clarke et al., 1970). 4-Cinn on the other hand is not a glial toxin, but instead, specifically blocks monocarboxylate transporters (MCT1 and MCT2) found on glial cells and neurons respectively (Dringen et al., 1993, McKenna et al., 2001).

4.2 Impact of glial cells – FC studies

FC is selectively taken up by glial cells and has limited neuronal toxicity unless the exposure is longer than 8 hours (Largo et al., 1996; Erlichman et al., 1998). As our exposure of neurons to FC was generally less than 2 hours, neuronal destruction was of limited concern. We rationalized that if lactate produced by glial

cells was responsible for the acidification, then by using FC we would be able to alter or blunt the acidification seen during hypoxia. We were also able to ensure that FC was having the intended effect because studies have shown that, with administration of FC, the RTN ECF pH will acidify (Erlichman et al., 1998). Although the exact source of this acidification is unknown, we postulated that this acidification of ECF pH will cause an acidification of neuronal pH. Hence, once FC was administered we expected the neuronal pH to acidify indicating that FC was having the intended effect.

During this study the neurons of the NTS did not acidify with FC but those of the RTN showed a significant acidification. We propose that this acidification of the RTN neurons was due to an extracellular acidification that occurs as a result of FC compromising the glia. We suggest that the neurons of the NTS did not acidify in response to FC because at this particular age (P1-P12), the NTS is relatively devoid of glial cells. This has been shown in a study performed by Erlichman and others whereby they stained both the RTN and NTS regions for glial fibrillary acidic protein (GFAP) and showed that the RTN contained far more glial cells than the NTS (Erlichman et al., 2004). Not only did the RTN have significantly more glial cells than the NTS but the NTS had very few glial cells.

However, the focus of these experiments was not on the difference between the NTS and RTN regions but on the impacts of glial cells on the hypoxia-induced neuronal acidification. This study showed that FC did not affect the magnitude of the hypoxia-induced acidification in either RTN or NTS regions of the brainstem (Figure 10). We can conclude a few things from these experiments. First, selective poisoning of the glial cells does not seem to alter the neuronal acidification seen during a

hypoxic bout in either RTN or NTS regions. This suggests that the glial cells are not the source of the lactic acid we propose is causing the hypoxia-induced acidification. Second, neurons of the NTS do not acidify during exposure to FC whereas those of the RTN do. We suggest that this can be attributed to the distribution of glial cells at this particular age. This second conclusion only helps to exclude glial cells as having an impact on the hypoxia induced acidification. If the NTS has very few glia, the glia are unlikely to be the source of lactic acid.

4.3 Impact of the Glial cells - 4-Cinn studies

In order to strengthen the conclusion that glial cells are not involved in the hypoxia induced acidification, 4-Cinn was used. As previously mentioned 4-Cinn is not a glial toxin, but at the correct concentrations will block both MCT1 and MCT2 transporters on neurons and glial cells. This would allow us to conclude that the hypoxia induced acidification was not due to lactate produced by glial cells. According to Erlichman and others, in the basal state glial cells are constantly sending lactate to the neurons for additional substrate. Using 4-Cinn they were able to block this flux of lactate which essentially alkalinized the neurons and acidified the glial cells (Erlichman et al., 2005). Using these findings, we can once again assume that 4-Cinn had the proposed effect based upon whether it alkalinized the neurons during control periods. We did not observe this alkalinization in the neurons of the RTN or the NTS (Figure 9). In addition to this, the hypoxia induced acidification seen under 4-Cinn conditions was not different from the control hypoxic exposure in either region.

The latter result is consistent with those experiments performed with FC; however the former result suggests one of two things. Either the 4-Cinn does not alkalinize neurons in a similar fashion to that of FC or the 4-Cinn did not effectively inhibit the glial MCT transporters. Due to the fact that there is very little evidence in the literature to suggest that 4-Cinn alkalinizes neurons while blocking the MCT transporters, we can only assume that the 4-Cinn was having the intended effect. These findings, along with those from FC, lead us to ultimately conclude that the glial cells do not seem to contribute to the hypoxia induced acidification seen in the neurons of the NTS and RTN.

4.6 Studies of reactive oxygen species (ROS)

We turned to ROS for the final portion of the study. For a long time, it has been well known that increases in the partial pressure of oxygen will increase the quantity of ROS produced in a variety of tissues (see Jamieson et al., 1986 for review). In fact, the most popular current theory suggests that during periods of hypoxia, it is the re-oxygenation of the tissues following the hypoxic bout that accounts for a significant increase in ROS production (Tan et al., 1999, Kloner et al., 1983, Darley-Usmar et al., 1991). We propose in this study that the increase in ROS occurs during the hypoxic bout itself prior to reoxygenation. Studies have recently shown that during a hypoxic bout, the quantities of ROS actually increase during the bout itself and not necessarily following the re-oxygenation (Magalhaes et al., 2005, Becker et al., 1999). Although the exact mechanism as to how ROS increases during hypoxia has not been identified, a suggestion can been made. Studies performed by Chandel and others show that during hypoxia the cytochrome complex III enzyme of

the mitochondrial electron transport chain produces superoxide (Chandel et al., 2000). Chandel proposes that this increase in superoxide is a message for the cell to produce hypoxia-inducible factor 1 which in turn stimulates the cell to produce certain gene products to counteract the hypoxia. Regardless, it has been shown that ROS increases during hypoxia.

In addition to showing that ROS increases during hypoxia, our study is directed at showing a relationship between increases in ROS and the hypoxia-induced acidification. We focused on ROS because studies in our lab have shown the ROS-generating compounds hydrogen peroxide and dihydroxyfumaric acid, and the chemical oxidants Chloramine-T and N-chlorosuccinimide, cause an intracellular acidification in neurons of the NTS (Mulkey et al., 2004). A variety of other studies have also shown intracellular acidifications in different cells in response to ROS (Tsai et al., 1997; Hu et al., 1998; Chao et al., 2002). The relationship between ROS and decreased pH_i is still being studied but some studies suggest a few possibilities as to how ROS causes an intracellular acidification. One possible option is that oxidative stress causes oxidation of cysteine and methionine residues of the Na^+/H^+ exchanger which renders it unable to control intracellular pH (Mulkey et al., 2004, Hu et al., 1998). Another possibility is that ROS could block oxidative phosphorylation which leads to an accumulation of lactic acid due to negative feedback. ROS has been shown to block oxidative phosphorylation (Chance and Boveris, 1978) and there is also some evidence that oxidative stress increases lactic acid production (Chan et al., 1982). Based upon all of the aforementioned studies, we focused on ROS for the second portion of this study.

4.7 Measurements of ROS during hypoxia

We tested our ROS theory using the superoxide specific ROS probe Dihydroethidium (DHE), which can be used to measure the relative quantities of intracellular superoxide produced. We found that the quantities of ROS actually increased during the hypoxic bouts as opposed to during the re-oxygenation (Figure 12). Due to the fact that the exposure of DHE is irreversible, we expected that once the levels of ROS increased, they would remain increased but interestingly the levels reduced during reoxygenation. Unlike the pH probe BCECF, DHE is not confined to the intracellular compartment. We therefore attribute the decreases in ROS to slow leakage of the DHE probe out of the cell. We assumed that not all of the probe leaks out of the cell instantaneously and as a result we will still see increases in ROS during further exposure to hypoxia. In addition, we assume that not all of the probe is excited during any one hypoxic exposure and therefore we are still able to produce the same magnitude of change in ROS during each hypoxic bout . Further studies need to be done with this specific probe to isolate the exact mechanics of the probe but the increase in superoxide that we observed during hypoxia is still a significant finding. Subsequently, these results provided us with a model for more experiments to relate ROS with the acidification seen during hypoxia.

4.8 Melatonin and MnTMPyp effects on ROS and pH_i

Using the increase in ROS during a hypoxic exposure as a control response, we repeated the hypoxic bout in the presence of two different ROS scavengers, melatonin and MnTMPyp. In both cases, the melatonin and MnTMPyp blunted the increase in ROS during a hypoxic bout (Figure 13 and 14). To then tie these ROS

findings to the acidification, we switched back to using the pH fluorescent probe BCECF. We monitored the pH_i response during the normal hypoxic exposure and then compared it to the acidification seen with hypoxia in conjunction with a cocktail of melatonin and MnTMPyp. We found that the acidification was still present during hypoxia in conjunction with the cocktail but it was decreased by approximately 20% which was statistically significant.

As previously mentioned a variety of mechanisms can be suggested as to how ROS is related to the hypoxia-induced acidification. Based upon other studies, we propose that hypoxia causes an increase in ROS by causing the cytochrome complex III enzyme to produce superoxide. This superoxide can potentially oxidize the cysteine and methionine residues of the Na^+/H^+ exchanger leading to an inability of the neuron to maintain intracelllular pH. It is also possible that the superoxide causes an increase in the production of lactic acid by blocking oxidative phosphorylation.

In summary it seems that the exposure of neurons of the NTS and RTN to bouts of hypoxia produces a robust acidification. We propose that this acidification is due to multiple factors which include increased lactic acid and ROS production. The primary controlling influence for this acidification is lactic acid produced by the neurons as opposed to the glia. ROS does seem to be involved in the acidification however the mechanism remains to be identified.

CHAPTER VI

FUTURE DIRECTIONS

A variety of future studies can be suggested to follow this project. Based upon work done by Erlichman and others (Erlichman et al., 2004), we propose studies which involve staining the NTS with GFAP as the rat ages from P1 onwards. The purpose of these studies would be to clarify whether the NTS region eventually develops a significant amount of glial cells and at what age this occurs. The other known chemosensitive regions could also be stained for glial cells and compared to that of the NTS and RTN.

Along the same lines, other chemosensitive regions such as the medullary raphe or Pre-Botzinger could be loaded with BCECF and the pH monitored during exposure to hypoxia. Comparing the pH responses of these regions to hypoxia to that of the NTS, this could perhaps suggest whether all of these regions have the same acidification or whether the NTS or RTN are alone in this response. In addition to this, electrophysiological recordings could be made at the same time as monitoring the pH_i change in several of these regions. In doing so, a more comprehensive study of the response of some of these regions to hypoxia can be done.

Another potential opportunity to study the effects of lactate would be to use lactate assays during repetitive bouts of hypoxia. These could potentially correlate with the findings from this study that indicate that lactate increases during a hypoxic bout and that this accounts for the hypoxia induced acidification.

Another potential avenue of study could involve using a pH clamping technique currently being performed in our lab. By clamping pH not only can we study the effects of CO2 independently of pH changes but perhaps also study those few hypoxia sensitive neurons found in the Pre-Botzinger complex and NTS and

illicit whether these neurons are responding to the oxygen itself or the acidification induced by hypoxia.

All of the studies in this project were performed in a superfusion chamber with single sided perfusion. In other words, the slice was placed on a flat glass coverslip and a nylon grid was used to immobilize it. The neurons that were visualized were those on the underside of the slice in which case, perfusion with aCSF was not equal to those neurons on the top portion of the slice. In this scenario, there is potential for byproducts of anaerobic metabolism, namely lactate, to build up on the underside of the slice. Using a second nylon grid underneath the slice and visualizing from the top of the slice could perhaps yield different results. Perhaps due to the fact that double sided perfusion can remove lactate more rapidly, the acidification during hypoxia will not be as robust. Perhaps, the lactate that produces the acidification is locked into the intracellular compartment and will still produce the same response. The increase in ROS could also be altered via double sided perfusion. These questions and others can be answered if a double sided perfusion system were to be used.

CHAPTER VII

BIBLIOGRAPHY

Agusti, A.G.N., 2005. Systemic effects of chronic obstructive pulmonary disease. *Proceedings of the American Thoracic Society.* vol. 2, no. 4: 367-70; discussion 371-2.

Andersson, U., Leighton, B., Young, M.E., Blomstrand, E., Newsholme, E.A., 1998. Inactivation of aconitase and oxoglutarate dehydrogenase in skeletal muscle in vitro by superoxide anions and/or nitric oxide. *Biochemical and Biophysical Research Communications.* vol. 249, no. 2: 512-6.

Attwell, D., Laughlin, S.B., 2001. An energy budget for signaling in the grey matter of the brain. *Journal of Cerebral Blood Flow Metabolism*. 21:1133–45.

Badr, A.E., Yin, W., Mychaskiw, G., Zhang, J. H., 2001. Dual effect of HBO on cerebral infarction in MCAO rats. *American Journal of Physiology. Regulatory, Integrative and Comparative Physiology.* vol. 280, no. 3: R766-70.

Ballanyi, K., 2004. Protective role of neuronal KATP channels in brain hypoxia. *The Journal of Experimental Biology.* vol. 207, no. Pt 18: 3201-12.

Becker, L.B., Vanden Hoek, T.L., Shao, Z.H., Li, C.Q., Schumacker, P.T., 1999. Generation of superoxide in cardiomyocytes during ischemia before reperfusion. *The American Journal of Physiology.* vol. 277, no. 6 Pt 2: H2240-6.

Bergamini, C.M., Gambetti, S., Dondi, A., Cervellati, C., 2004. Oxygen, reactive oxygen species and tissue damage. *Current pharmaceutical design.* vol. 10, no. 14: 1611-26.

Bisgard, G.E., Neubauer J.A., 1995. Peripheral and central effects of hypoxia. In Dempsey JA, Pack AI (eds): Regulation of Breathing. New York: Marcel Dekker, pp 617-668.

Brahma, B., Forman, R.E., Stewart, E.E., Nicholson, C. and Rice, M.E., 2000. Ascorbate inhibits edema in brain slices. *Journal of Neurochemistry*. 74, 1263–1270.

Bright, G.R., Fisher, G.W., Rogowska, J., Taylor, D.L., 1989. Fluorescence ratio imaging microscopy. In D.L. Taylor and Y.L. Wang (Eds.) Fluorescence Microscopy of Living Cells in Culture part B, Quantitative Fluorescence Microscopy, Imaging and Spectroscopy, Academic Press, San Diego, CA, pp. 157-190.

Chambers-Kersh, L., Ritucci, N.A., Dean, J.B., Putnam, R.W., 2000. Response of intracellular pH to acute anoxia in individual neurons from chemosensitive and nonchemosensitive regions of the medulla. *Advances in Experimental Medicine and Biology*. vol. 475: 453-64.

Chan, P.H., Yurko, M., Fishman, R.A., 1982. Phospholipid degradation and cellular edema induced by free radicals in brain cortical slices. *Journal of Neurochemistry.* vol. 38, no. 2: 525-31.

Chandel, N.S., McClintock, D.S., Feliciano, C.E., Wood, T.M., Melendez, J.A., Rodriguez, A.M., Schumacker, P.T., 2000. Reactive oxygen species generated at mitochondrial complex III stabilize hypoxia-inducible factor-1alpha during hypoxia: a mechanism of O_2 sensing. *The journal of biological chemistry*. vol 275, no. 33: 25130-8.

Chance, B., Boveris, A. Hyperoxia and hydroperoxide metabolism. *Extra-Pulmonary Manifestations of Respiratory Disease, edited by Robin E. New York: Dekker*, 1978, p. 185–238.

Chao, C., Jin, J., Tsai, C., Tsai, Y., Chen, W., Chung, C., Loh, S., 2002. Effect of hydrogen peroxide on intracellular pH in the human atrial myocardium. *The Chinese Journal of Physiology.* vol. 45, no. 3: 123-9.

Chen, M. and Simard, J.M., 2001. Cell swelling and a nonselective cation channel regulated by internal Ca^{2+} and ATP in native reactive astrocytes from adult rat brain. *Journal of Neuroscience*. 21, 6512–6521.

Clarke D.D., Nicklas W.J., Berl S., 1970. Tricarboxylic acid-cycle metabolism in brain: effect of fluoroacetate and fluorocitrate on the labeling of glutamate, aspartate, glutamine and y-aminobutyrate. *Biochem Journal.* vol. 120:345-351

Connelly, C.A., Ellenberger H.H., Feldman J.L., 1990. Respiratory activity in the retrotrapezoid nucleus in cat. *American. Journal of Physiology.* vol. 258, no. 2 Pt 1: L33-44.

Darley-Usmar, V.M., Stone, D., Smith, D., Martin, J.F., 1991. Mitochondria, oxygen and reperfusion damage. *Annals of medicine.* vol. 23, no. 5: 583-8.

Dean, J.B., Lawing, W.L., Millhorn, D.E., 1989. CO_2 decreases membrane conductance and depolarizes neurons in the nucleus tractus solitarii. *Experimental Brain Research*. vol. 76, no. 3: 656-61.

Deitmer, J.W., Rose, C.R., 1996. pH regulation and proton signalling by glial cells. *Progress in Neurobiology.* vol. 48, no. 2: 73-103.

Dringen, R., Wiesinger, H., Hamprecht, B., 1993. Uptake of L-lactate by cultured rat brain neurons. *Neuroscience Letters.* vol. 163, no. 1: 5-7.

Erecinska, M., Silver, I.A., 1990. Metabolism and role of glutamate in mammalian brain. *Progress in Neurobiology.* vol. 35, no. 4: 245-96.

Erlichman, J.S., Cook, A., Schwab, M.C., Budd, T.W., Leiter, J.C., 2004. Heterogeneous patterns of pH regulation in glial cells in the dorsal and ventral medulla. *American Journal of Physiology. Regulatory, Integrative and Comparative Physiology.* vol. 286, no. 2: R289-302.

Erlichman, J.S., Hewitt-Higgins, A., Hart M.P., Leiter, J.C., 2005. The ventilatory effects of impaired astrocytic – neuronal lactate shuttle in the rat. Program No. 636.13. Abstract Viewer/Itinerary Planner. Washington, DC: Society for Neuroscience.

Erlichman, J.S., Li, A., Nattie, E.E., 1998. Ventilatory effects of glial dysfunction in a rat brain stem chemoreceptor region. *Journal of Applied Physiology.* vol. 85, no. 5: 1599-604.

Even, S., Garrigues, C., Loubiere, P., Lindley, N.D., Cocaign-Bousquet, M., 1999. Pyruvate metabolism in Lactococcus lactis is dependent upon glyceraldehyde-3-phosphate dehydrogenase activity. *Metabolic engineering.* vol. 1, no. 3: 198-205.

Filosa, J.A., Dean, J.B., Putnam, R.W., 2002. Role of intracellular and extracellular pH in the chemosensitive response of rat locus coeruleus neurones. *The Journal of physiology.* vol. 541, no. Pt 2: 493-509.

Fletcher, E.C., 2003. Sympathetic over activity in the etiology of hypertension of obstructive sleep apnea. *Sleep*. 26, no. 1: 15-9.

Gale, S.D., Hopkins, R.O., 2004. Effects of hypoxia on the brain: Neuroimaging and neuropsychological findings following carbon monoxide poisoning and obstructive sleep apnea. Journal *of the International Neuropsychological Society*. vol. 10, no. 1: 60-71.

Gasser, U.E., Hatten, M.E., 1990. Central nervous system neurons migrate on astroglial fibers from heterotypic brain regions in vitro. *Proceedings of the National Academy of Sciences of the United States of America.* vol. 87, no. 12: 4543-7.

Girotti, A.W., 1998. Lipid hydroperoxide generation, turnover, and effector action in biological systems. *Journal of Lipid Research.* vol. 39, no. 8: 1529-42.

Gonzalez C., Almaraz L., Obeso A., Rigual R., 1992. Oxygen and acid chemoreception in the carotid body chemoreceptors. *Trends in Neurosciences*. vol. 15, no. 4: 146-53.

Graziewicz, M.A., Day, B.J., Copeland, W.C., 2002. The mitochondrial DNA polymerase as a target of oxidative damage. *Nucleic Acids Research.* vol. 30, no. 13: 2817-24.

Guyenet, P.G., Stornetta, R.L., Bayliss, D.A., Mulkey, D.K., 2005. Retrotrapezoid nucleus: a litmus test for the identification of central chemoreceptors. *Experimental physiology.* vol. 90, no. 3: 247-53; discussion 253-7.

Harada, Y., Kuno, M., Wang, Y.Z., 1985. Differential effects of carbon dioxide and pH on central chemoreceptors in the rat in vitro. *The Journal of Physiology.* vol. 368: 679-93.

Hampton, M.B., Kettle, A.J., 1996. Involvement of superoxide and myeloperoxidase in oxygen-dependent killing of Staphylococcus aureus by neutrophils. *Infection and immunity.* vol. 64, no. 9: 3512-7.

Hu, Q., Xia, Y., Corda, S., Zweier, J.L., Ziegelstein, R.C., 1998. Hydrogen peroxide decreases pH_i in human aortic endothelial cells by inhibiting Na^+/H^+ exchange. *Circulation Research.* vol. 83, no. 6: 644-51.

Hill, G.B., Osterhout, S., 1972. Experimental effects of hyperbaric oxygen on selected clostridial species. I. In-vitro studies. *The Journal of infectious diseases.* vol. 125, no. 1: 17-25.

Izumi, Y., Katsuki, H., Zorumski, C.F., 1997. Monocarboxylates (pyruvate and lactate) as alternative energy substrates for the induction of long-term potentiation in rat hippocampal slices. *Neuroscience letters.* vol. 232, no. 1: 17-20.

Jamieson, D., Chance, B., Cadenas, E., Boveris, A., 1986. The relation of free radical production to hyperoxia. Annual Review of Physiology. vol. 48: 703-19.

Joyeux-Faure, M., Stanke-Labesque, F., Lefebvre, B., Beguin, P., Godin-Ribuot, D., Ribuot, C., Launois, S.H., Bessard, G., Levy, P., 2005. Chronic intermittent hypoxia increases infarction in the isolated rat heart. *Journal of Applied Physiology*. vol. 98, no. 5: 1691-6.

Katz-Salamon, M., 2004. Delayed chemoreceptor responses in infants with apnoea. *Archives of Disease in Childhood.* vol. 89, no. 3: 261-6.

Kulik, A., Brockhaus, J., Pedarzani, P., Ballanyi, K., 2002. Chemical anoxia activates ATP-sensitive and blocks Ca(2+)-dependent K(+) channels in rat dorsal vagal neurons in situ. *Neuroscience.* vol. 110, no. 3: 541-54.

Kiwull-Schone, H., Kiwull, P., 1992. Hypoxia and the "reaction theory" of central respiratory chemosensitivity. *Advances in Experimental Medicine and Biology*. vol. 316: 347-57.

Killilea, D.W., Hester, R., Balczon, R., Babal, P., Gillespie, M.N., 2000. Free radical production in hypoxic pulmonary artery smooth muscle cells. *American Journal of Physiology. Lung Cellular and Molecular Physiology.* vol. 279, no. 2: L408-12.

Kloner, R. A., Ellis, S.G., Carlson, N.V., Braunwald, E., 1983. Coronary reperfusion for the treatment of acute myocardial infarction: postischemic ventricular dysfunction. *Cardiology.* vol. 70, no. 5: 233-46.

Knighton, D.R., Halliday, B., Hunt, T.K., 1986. Oxygen as an antibiotic. A comparison of the effects of inspired oxygen concentration and antibiotic administration on in vivo bacterial clearance. *Archives of surgery.* vol. 121, no. 2: 191-5.

Largo, C., Cuevas, P., Somjen, G.G., Martin del Rio, R., Herreras, O., 1996. The effect of depressing glial function in rat brain in situ on ion homeostasis, synaptic transmission, and neuron survival. *The Journal of neuroscience: the official journal of the Society for Neuroscience.* vol. 16, no. 3: 1219-29.

Lavie, L., 2005. Sleep-disordered breathing and cerebrovascular disease: a mechanistic approach. *Neurologic Clinics.* vol. 23, no. 4: 1059-75.

Levi, G., Gallo, V., Cohen, J., 1986. Astrocyte subpopulations and glial precursors in rat cerebellar cultures. *Adv Biosci.* 61:21-30.

Li, A., Nattie, E.E., 1997. Focal central chemoreceptor sensitivity in the RTN studied with a CO_2 diffusion pipette in vivo. *Journal of applied physiology.* vol. 83, no. 2: 420-8.

Loaiza, A., Porras, OH., Barros, LF., 2003. Glutamate triggers rapid glucose transport stimulation in astrocytes as evidenced by real-time confocal microscopy. *Journal of Neuroscience*. vol. 23, no. 19: 7337-42.

Magalhaes, J., Ascensao, A., Soares, J.M.C., Ferreira, R., Neuparth, M.J., Marques, F., Duarte, J.A., 2005. Acute and severe hypobaric hypoxia increases oxidative stress and impairs mitochondrial function in mouse skeletal muscle. *Journal of Applied Physiology.* vol. 99, no. 4: 1247-53.

MacGregor, D.G., Avshalumov, M.V., Rice, M.E., 2003. Brain edema induced by in vitro ischemia: causal factors and neuroprotection, *Journal of Neurochemistry.* 85, 1402-1411.

McKenna, M.C., Hopkins, I.B., Carey, A., 2001. Alpha-cyano-4-hydroxycinnamate decreases both glucose and lactate metabolism in neurons and astrocytes: implications for lactate as an energy substrate for neurons. *Journal of neuroscience research.* vol. 66, no. 5: 747-54.

Miles, R., 1983. Does low pH stimulate central chemoreceptors located near the ventral medullary surface?. *Brain Research.* vol. 271, no. 2: 349-53.

Muhvich, K. H., Park, M. K., Myers, R. A., Marzella, L., 1989. Hyperoxia and the antimicrobial susceptibility of Escherichia coli and Pseudomonas aeruginosa. *Antimicrobial agents and chemotherapy.* vol. 33, no. 9: 1526-30.

Mulkey, D.K., Henderson, R.A., 3rd., Putnam, R.W., Dean, J.B., 2003. Hyperbaric oxygen and chemical oxidants stimulate CO2/H+-sensitive neurons in rat brain stem slices. *Journal of applied physiology.* vol. 95, no. 3: 910-21.

Mulkey, D.K., Henderson, R.A. 3rd., Ritucci, N.A., Putnam, R.W., Dean, J.B., 2004. Oxidative stress decreases pHi and Na(+)/H(+) exchange and increases excitability of solitary complex neurons from rat brain slices. *American journal of physiology. Cell physiology.* vol. 286, no. 4: C940-51.

Muller, M., Ballanyi, K., 2003. Dynamic recording of cell death in the in vitro dorsal vagal nucleus of rats in response to metabolic arrest. *Journal of neurophysiology.* vol. 89, no. 1: 551-61.

Narkiewicz, K., Somers, V. K., 2003. Sympathetic nerve activity in obstructive sleep apnoea. *Acta physiologica Scandinavica.* vol. 177, no. 3: 385-90.

Nattie, E., 1999. CO_2, brainstem chemoreceptors and breathing. *Progress in Neurobiology*. vol. 59, no. 4: 299-331.

Nattie, E.E., 2000. Multiple sites for central chemoreception: their roles in response sensitivity and in sleep and wakefulness. *Respiratory Physiology.* 122, 223-235.

Nattie, E.E., 1998. Central Chemoreceptors, pH, and Respiratory Control. In: Kaila, K., Ransom, B.R., (Ed.). pH and Brain Function. Wiley-Liss, New York, pp. 535-560

Nehlig, A., Wittendorp-Rechenmann, E., Lam, CD., 2004. Selective uptake of [14C]2-deoxyglucose by neurons and astrocytes: high-resolution microautoradiographic imaging by cellular 14C-trajectography combined with immunohistochemistry. *Journal of Cerebral Blood Flow and Metabolism*. vol. 24, no. 9: 1004-14.

Neubauer, J.A., Gonsalves, S.F., Chou, W., Geller, H.M., Edelman, N.H., 1991. Chemosensitivity of medullary neurons in explant tissue cultures. *Neuroscience*. vol. 45, no. 3: 701-8.

Neubauer, J.A., Sunderram, J., 2004. Oxygen-sensing neurons in the central nervous system. *Journal of applied physiology.* vol. 96, no. 1: 367-74.

Orkand R.K., 1986. Introductory remarks: Glial-interstitial fluid exchange. *Ann NY Acad Sci.* 481:269-72.

Paulsen, R.E., Contestabile, A., Villani, L. and Fonnum, F., 1987. An in vivo model for studying function of brain tissue temporarily devoid of glial cell metabolism: the use of fluorocitrate, *Journal of Neurochemistry*. 48, 1377-1385.

Pascual, O., Morin-Surun, M.P., Barna, B., Denavit-Saubie´, M., Peqquignot, J.M., Champagnat J., 2002. Progesterone reverses the neuronal responses to hypoxia in rat nucleus tractus solitarius in vitro. *Journal of Physiology.* 544: 511–520.

Pellerin, L., Magistretti, P.J., 1994. Glutamate uptake into astrocytes stimulates aerobic glycolysis: a mechanism coupling neuronal activity to glucose utilization. *Proceedings of the National Academy of Sciences of the United States of America*. vol. 91, no. 22: 10625–9.

Pellerin, L., Magistretti, P.J., 2004. Neuroenergetics: calling upon astrocytes to satisfy hungry neurons. *The Neuroscientist: A review journal bringing neurobiology, neurology and psychiatry*. vol. 10, no. 1: 53-62.

Pierre, K., Pellerin, L., Debernardi, R., Riederer, B.M., Magistretti, P. J., 2000. Cell-specific localization of monocarboxylate transporters, MCT1 and MCT2, in the adult mouse brain revealed by double immunohistochemical labeling and confocal microscopy. *Neuroscience*. vol. 100, no. 3: 617-27.

Putnam, R.W, Filosa, J.A, Ritucci, N.A., 2004. Cellular mechanisms involved in CO_2 and acid signaling in chemosensitive neurons. *American Journal of Physiology. Cell Physiology*. vol. 287, no. 6: C1493-526.

Putnam, R.W., Grubbs, R.D., 1990. Steady-state pH_i, buffering power, and effect of CO_2 in a smooth muscle cell line. *American Journal of Physiology*. vol. 258, C461-C469.

Raphael, J. C., Elkharrat, D., Jars-Guincestre, M. C., Chastang, C., Chasles, V., Vercken, J. B., Gajdos, P., 1989. Trial of normobaric and hyperbaric oxygen for acute carbon monoxide intoxication. *Lancet.* vol. 2, no. 8660: 414-9.

Reichert, S.A., Kim-Han, J.S. and Dugan, L.L., 2001. The mitochondrial permeability transition pore and nitric oxide synthase mediate early mitochondrial depolarization in astrocytes during oxygen-glucose deprivation. *Journal of Neuroscience*. 21, 6608–6616.

Richerson, G.B., 1995. Response to CO2 of neurons in the rostral ventral medulla in vitro. *Journal of neurophysiology*. vol. 73, no. 3: 933-44.

Ritucci, N. A., Erlichman J.S., Dean J.B, Putnam R.W., 1996. A fluorescence technique to measure intracellular pH of single neurons in the brainstem slices, *Journal of Neuroscience Methods*. 68, 149-163.

Ritucci, N.A., Erlichman, J.S., Leiter, J.C., Putnam, R.W., 2005. Response of membrane potential and intracellular pH to hypercapnia in neurons and astrocytes from rat retrotrapezoid nucleus. *American journal of physiology. Regulatory, integrative and comparative physiology.* vol. 289, no. 3: R851-61.

Schneider, U., Poole, R.C., Halestrap, A.P., Grafe, P., 1993. Lactate-proton co-transport and its contribution to interstitial acidification during hypoxia in isolated rat spinal roots. *Neuroscience*. vol. 53, no. 4: 1153-62.

Smith, C.A., Engwall, M.J., Dempsey, J.A., Bisgard, G.E., 1993. Effects of specific carotid body and brain hypoxia on respiratory muscle control in the awake goat. *The Journal of Physiology.* vol. 460: 623-40.

Smith, D., Pernet, A., Hallett, W.A., Bingham, E., Marsden, P.K., Amiel, S.A., 2003. Lactate: a preferred fuel for human brain metabolism in vivo. *Journal of Cerebral Blood Flow Metabolism*. vol. 23, no. 6: 658-64.

Solomon, I.C., Edelman, N.H., O'Neal, M.H., 2000. CO(2)/H(+) chemoreception in the cat pre-Botzinger complex in vivo. *Journal of applied physiology.* vol. 88, no. 6: 1996-2007.

Solomon, I.C., Edelman, N.H., Neubauer, J.A., 2000. The pre-Botzinger complex functions as a central hypoxia chemoreceptor for respiration in vivo. *Journal of Neurophysiolgy.* 83: 2854–2868.

Tan, S., Zhou, F., Nielsen, V.G., Wang, Z., Gladson, C.L., Parks, D.A., 1999. Increased injury following intermittent fetal hypoxia-reoxygenation is associated with increased free radical production in fetal rabbit brain. *Journal of neuropathology and experimental neurology.* vol. 58, no. 9: 972-81.

Thom, S. R., Taber, R. L., Mendiguren, I. I., Clark, J. M., Hardy, K. R., Fisher, A. B., 1995. Delayed neuropsychologic sequelae after carbon monoxide poisoning: prevention by treatment with hyperbaric oxygen. *Annals of emergency medicine.* vol. 25, no. 4: 474-80.

Thomas, J.A., Buchsbaum, R.N., Zimniak, A., Racker, E., 1979. Intracellular pH measurements in Ehrlich ascites tumor cells utilizing spectroscopic probes generated in situ. *Biochemistry.* vol. 18, no. 11: 2210-8.

Tibbles, P.M., Edelsberg, J.S., 1996. Hyperbaric-oxygen therapy. *The New England Journal of Medicine*. vol. 334, no. 25: 1642-8.

Tsai, K.L., Wang, S.M., Chen, C.C., Fong, T.H., Wu, M.L., 1997. Mechanism of oxidative stress-induced intracellular acidosis in rat cerebellar astrocytes and C6 glioma cells. *The Journal of Physiology.* vol. 502, Pt 1: 161-74.

Véga, C., Martiel, JL., Drouhault, D., Burckhart, MF., Coles, J.A., 2003. Uptake of locally applied deoxyglucose, glucose and lactate by axons and Schwann cells of rat vagus nerve. *Journal of Physiology.* vol 546, no. Pt 2: 551–64.

Walz, W., Mukerji, S., 1988. Lactate release from cultured astrocytes and neurons: a comparison. *Glia*.vol. 1, no. 6: 366-70.

Wei, Y., Lee, H., 2002 Oxidative stress, mitochondrial DNA mutation, and impairment of antioxidant enzymes in aging. *Experimental Biological Medicine.* vol. 227, no. 9: 671-82.

Wellner-Kienitz, M.C., Shams, H., 1998. CO2-sensitive neurons in organotypic cultures of the fetal rat medulla. *Respiration physiology.* vol. 111, no. 2: 137-51.

Wu, M.L., Tsai, K.L., Wang, S.M., Wu, J.C., Wang, B.S., Lee, Y.T., 1996. Mechanism of hydrogen peroxide and hydroxyl free radical-induced intracellular acidification in cultured rat cardiac myoblasts. *Circulation Research*. vol. 78, no 4:564-72.

Xu, W., Chi, L., Row, B.W., Xu, R., Ke, Y., Xu, B., Luo, C., Kheirandish, L., Gozal, D., Liu, R., 2004. Increased oxidative stress is associated with chronic intermittent hypoxia-mediated brain cortical neuronal cell apoptosis in a mouse model of sleep apnea. *Neuroscience.* vol. 126, no. 2: 313-23.

Yin, D., Zhang, J.H., 2005. Delayed and multiple hyperbaric oxygen treatments expand therapeutic window in rat focal cerebral ischemic model. *Neurocritical Care.* vol. 2, no. 2: 206-11.